

CONTROLLED RELEASE OF FIBROIN REPEAT-TAGGED PROTEINS FROM SILK HYDROGEL



A Dissertation Submitted in Partial Fulfillment of the Requirements  
for the Degree of Doctor of Philosophy in Biochemistry and Molecular Biology

Department of Biochemistry

FACULTY OF SCIENCE

Chulalongkorn University

Academic Year 2020

Copyright of Chulalongkorn University

การปลดปล่อยแบบควบคุมของโปรตีนที่เชื่อมกับส่วนซ้ำไฟโบรอินใหม่จากไฮโดรเจล



วิทยานิพนธ์นี้เป็นส่วนหนึ่งของการศึกษาตามหลักสูตรปริญญาวิทยาศาสตรดุษฎีบัณฑิต  
สาขาวิชาชีวเคมีและชีววิทยาโมเลกุล ภาควิชาชีวเคมี  
คณะวิทยาศาสตร์ จุฬาลงกรณ์มหาวิทยาลัย  
ปีการศึกษา 2563  
ลิขสิทธิ์ของจุฬาลงกรณ์มหาวิทยาลัย



จตุรงค์ พรหมสุข : การปลดปล่อยแบบควบคุมของโปรตีนที่เชื่อมกับส่วนซ้ำไฟโบรอินใหม่จากไฮโดรเจล. ( CONTROLLED RELEASE OF FIBROIN REPEAT-TAGGED PROTEINS FROM SILK HYDROGEL ) อ.ที่ปรึกษาหลัก  
: อ. ดร.กิตติคุณ ว่างานนท์, อ.ที่ปรึกษาร่วม : อ. ดร.พีรพัฒน์ ทองนิก

โปรตีนชีวภาพที่มีคุณสมบัติเป็นยาอย่างเช่น Growth Factor มีบทบาทสำคัญในการแพทย์ปัจจุบัน โปรตีนชีวภาพนี้มีความสามารถในการกระตุ้นและซ่อมแซมเนื้อเยื่อเฉพาะจุด โดยนำ Growth factor นี้ร่วมกับโครงข่ายเซลล์เช่น ไฮโดรเจล จากนั้นนำเข้าสู่บริเวณที่ต้องการซ่อมแซม อย่างไรก็ตามการแพร่กระจายของ Growth factor ออกจากบริเวณที่ต้องการหรือระยะเวลาในการปลดปล่อยไม่เหมาะสมนั้น ก่อให้เกิดปัญหาต่างๆ เช่น การกระตุ้นการเกิดเนื้องอกในบริเวณต่างๆของร่างกาย หรือเกิดการอักเสบที่ควบคุมไม่ได้ ดังนั้นวัตถุประสงค์ของงานวิจัยนี้เพื่อสร้างแบบจำลองการแพร่ของโปรตีนชีวภาพจากไฮโดรเจลโดยใช้โปรตีนเรืองแสงสีเขียว (GFP) เป็นตัวแทนของโปรตีนชีวภาพและงานวิจัยนี้ใช้โปรตีนไฟโบรอิน (SF) จากไหมเป็นโครงข่ายของเซลล์ไฮโดรเจล ดังนั้นเพื่อศึกษาการปลดปล่อย GFP เป็นโปรตีนชีวภาพต้นแบบซึ่งมี SF เชื่อมติดอยู่ (SF-GFP) SF-GFP ที่สร้างขึ้นมีลำดับกรดอะมิโนในโปรตีน Silk fibroin ที่มีลำดับซ้ำๆ กันคือ (GAGAGS)<sub>n</sub> ลำดับกรดอะมิโนที่ซ้ำกันของโปรตีน SF เป็นส่วนที่ทำให้เกิดโครงสร้างแบบ  $\beta$ -sheet ภายในโปรตีน SF การศึกษาระยะเวลาของโปรตีน SF ขึ้นรูปเป็น hydrogel พบว่า SF-GFP ส่งผลให้โปรตีน SF ขึ้นรูปเป็น hydrogel ได้เร็วขึ้น การปลดปล่อยของ SF-GFP จาก SF hydrogel สามารถลดผลของการปลดปล่อยแบบรวดเร็วและรักษาระดับการปลดปล่อยอย่างต่อเนื่อง โดยเฉพาะอย่างยิ่ง SF-hydrogel ที่ประกอบด้วย 6 repeat units ของ silk นอกจากนี้ได้ศึกษาโครงสร้างของ SF hydrogel พบว่าไฮโดรเจล ที่ผสมด้วยโปรตีนของ SF ที่มีส่วนซ้ำที่ยาวขึ้นทำให้ปริมาณของ  $\beta$ -sheet เพิ่มขึ้น และยังส่งผลให้อัตราการย่อยสลายของไฮโดรเจลลดลงด้วย เมื่อศึกษาหลักการปลดปล่อยของ GFP ด้วยเทคนิค FTIR และ XRD พบว่าการปลดปล่อยของ GFP จาก SF hydrogel ไม่ได้ขึ้นอยู่กับปริมาณของ  $\beta$ -sheet ใน hydrogel โดยตรง แต่การปลดปล่อย GFP ขึ้นอยู่กับแรงยึดเหนี่ยวระหว่างโมเลกุลระหว่างส่วนซ้ำของ SF ที่สร้างขึ้นกับส่วนซ้ำ SF ของไฮโดรเจล ซึ่งยังมีส่วนซ้ำที่ยาวขึ้นก็จะมีแรงยึดเหนี่ยวระหว่างโมเลกุลที่แรงขึ้น จากผลการทดลองนี้ได้สร้างส่วนซ้ำของ SF ที่มี 6 ส่วนซ้ำเชื่อมติดกับ growth factor (bFGF) เพื่อนำมาประยุกต์ใช้ในงานวิศวกรรมเนื้อเยื่อ พบว่าเพปไทด์ที่สร้างขึ้นสามารถทำงานได้เมื่อนำมาทดสอบการเพิ่มขึ้นของเซลล์ NIH-3T3 ที่มีความเข้มข้นตั้งแต่ 10 ng/ml ขึ้นไป และจากการศึกษาการเพิ่มขึ้นของเซลล์ NIH-3T3 ต่อการปลดปล่อยของ bFGF จาก (GAGAGS)<sub>6</sub>-bFGF พบว่าเซลล์จะมีการเพิ่มขึ้นแบบค่อยเป็นค่อยไปและยังคงมีการเพิ่มขึ้นของเซลล์อย่างต่อเนื่อง ซึ่งจากผลการศึกษานี้เป็นผลมาจากส่วนซ้ำของ SF ช่วยควบคุมการปลดปล่อยของ bFGF

จุฬาลงกรณ์มหาวิทยาลัย  
CHULALONGKORN UNIVERSITY

สาขาวิชา ชีวเคมีและชีววิทยาโมเลกุล  
ปีการศึกษา 2563

ลายมือชื่อนิสิต .....  
ลายมือชื่อ อ.ที่ปรึกษาหลัก .....  
ลายมือชื่อ อ.ที่ปรึกษาร่วม .....

# # 5772806423 : MAJOR BIOCHEMISTRY AND MOLECULAR BIOLOGY

KEYWORD: silk fibroin repeat unit mimic peptide, GFP release profile, growth factor, tissue engineering  
 Jaturong Promsuk : CONTROLLED RELEASE OF FIBROIN REPEAT-TAGGED PROTEINS FROM SILK  
 HYDROGEL . Advisor: Kittikhun Wangkanont, Ph.D. Co-advisor: Peerapat Thongnuek, Ph.D.

Protein-based biologic drugs such as growth factors are playing important roles in modern medicine. These proteins can be used to stimulate local tissue repair. Growth factors are often incorporated into a scaffold, such as a hydrogel, and then put into the desired area of the body to achieve therapeutic effects. However, diffusion of these growth factors outside of the designated area or inappropriate release time can have deleterious consequences, such as inducing tumors in other areas of the body or uncontrolled inflammation. Therefore, this project aims to create a model to study diffusion of protein from hydrogel by using green fluorescent protein (GFP) as a biologics model and silk hydrogel as a scaffold to investigate the drug release behavior from the hydrogel. To investigate the bioactive release profile, GFP fused to silk repeating units (GAGAGS)<sub>n</sub>-GFP was used as a model. In this study, the gelation time of the silk fibroin hydrogel containing GFP is faster than the pure silk fibroin hydrogel. The release of (GAGAGS)<sub>n</sub>-GFP from silk fibroin hydrogel reduces the burst release effect and sustained release profile, especially silk fibroin hydrogel containing six repeats of SF tagged GFP. These results indicate that increasing the number of silk repeating unit(s) help sustain the model protein release from silk fibroin hydrogel. In addition, the release mechanism was investigated by FTIR and XRD method. The result showed that the release profile of GFP was not dependent on the  $\beta$ -sheet content of hydrogel but could be occur from hydrophobic interaction between repeating unit of peptide and repeating unit of SF hydrogel scaffold. After determining the optimal number of repeating units, the six repeating units tagged-basic fibroblast growth factor (bFGF) is produced and showed the function. The bFGF-incorporated hydrogel is examined for bFGF release and stimulated of cell proliferation in cell culture. These results indicate that six repeating units-tagged bFGF can sustain release of bFGF detected by NIH3T3 proliferation.

จุฬาลงกรณ์มหาวิทยาลัย  
 CHULALONGKORN UNIVERSITY

Field of Study: Biochemistry and Molecular Biology Student's Signature .....

Academic Year: 2020 Advisor's Signature .....

Co-advisor's Signature .....

## ACKNOWLEDGEMENTS

I would like to express my sincere thank and honor to my advisor, Dr. Kittikhun Wangkanont, for accepting me into his laboratory, Under his guidance, I have learned the way of research technical and planning, critical thinking and manuscript writing. I could have never imagined having better mentor for my PhD study. Besides my advisor, I express my thankfulness to my co-advisor, Dr. Peerapat Thongnuek, who inspires and encourages me to cheer up and improve myself during my study. My special gratitude is extended to the committee members: Assoc. Prof. Dr. Teerapong Buobucha, Assoc. Prof. Dr. Manchumas Prosunthron, Asst. Prof. Dr. Thanyada Rungrotmonkol for serving as progress and dissertation committee member. I got their kind and useful suggestions for improving my work. Special thanks to Asst. Prof. Dr. Chomdao Sinthuvanich, Biochemistry, Kasetsart University for serving as an external examiner.

I would like to acknowledge the professors, researchers, and technicians who have helped me since the beginning of my study. In addition, I would like to thanks both academic and supporting staffs of department of biochemistry, faculty of science, Chulalongkorn University for kind assistance and facility, and also many of services. I could not have completed my research without them.

My deepest thanks go to my family and friends who have always supported me. First, I would like to thank mom, sister, and my family. Their love, compassion, and support allows me to succeed today. I would like to thank all of my friends from Wangkanont's laboratory members, who have shared memories and support me when I have some trouble. And also to thank all of my friend in department for help me in everything. You guys made this long journey a lot more fun.

Finally, special thanks to the Science Achievement Scholarship of Thailand (SAST) for funding and service during my journey. I also thanks the 90th Aniversary of Chulalongkorn University Fund (Ratchadaphiseksomphot Endowment Fund) for patial support of the research expenses. This project might not be completed without their funding. Thank a lot for giving me a chance.

Jaturong Promsuk

## TABLE OF CONTENTS

	Page
.....	iii
ABSTRACT (THAI).....	iii
.....	iv
ABSTRACT (ENGLISH).....	iv
ACKNOWLEDGEMENTS.....	v
TABLE OF CONTENTS.....	vi
LIST OF TABLES.....	x
LIST OF FIGURES.....	xi
LIST OF ABBREVIATION.....	xiii
CHAPTER I INTRODUCTION.....	1
1.1 Rationales and Theories.....	1
1.2 Objective of this dissertation.....	8
1.3 Expected beneficial outcome from the dissertation.....	9
CHAPTER II LITERATURE.....	11
2.1 Control drug release system.....	11
2.2 Natural polymer-based CRS.....	14
2.2.1 Silk.....	14
2.2.2 Silk fibroin for control drug delivery system.....	19
2.2.3 Silk fibroin hydrogel for control drug release.....	21
2.3 Biomimetic peptide for control drug release.....	25
2.4 Control release of biosignalling on tissue engineering application.....	27

2.4.1 Biosinalling in tissue engineering .....	30
2.4.1.1 Basic fibroblast growth factor (bFGF).....	31
CHAPTER III METHODOLOGY.....	33
3.1 Construction of (GAGAGS) <sub>n</sub> -tagged GFP expression plasmid .....	33
3.2 (GAGAGS) <sub>n</sub> tagged GFP protein expression and purification .....	37
3.3 Preparation of silk fibroin solution .....	39
3.4 Silk fibroin gelation time detection .....	40
3.5 <i>In vitro</i> GFP release.....	41
3.6 <i>In vitro</i> enzymatic degradation of silk fibroin hydrogel.....	41
3.7 SF hydrogel structure characterization.....	42
3.7.1 Lyophilized silk fibroin assemble with (GAGAGS) <sub>n</sub> -GFP-H <sub>6</sub> peptide hydrogel .....	42
3.7.2 X-ray diffraction (XRD) of SF lyophilized gel .....	43
3.7.3 Fourier-transform infrared (FTIR) spectroscopy .....	43
3.8 Construction of (GAGAGS) <sub>n</sub> -tagged bFGF expression plasmid.....	43
3.9 bFGF and (GAGAGS) <sub>6</sub> -bFGF expression and purification .....	44
3.9.1 IPTG optimization for bFGF and (GAGAGS) <sub>6</sub> -bFGF expression.....	44
3.9.2 bFGF and (GAGAGS) <sub>6</sub> -bFGF expression using <i>Escherichia coli</i> Tuner (DE3).....	45
3.9.3 Purification of bFGF peptide expressed from pET28b-bFGF plasmid.....	46
3.9.4. Purification of bFGF and (GAGAGS) <sub>6</sub> -bFGF expressed from pMALc5x plasmid .....	48
3.10 Cell culture.....	50
3.11 Optimized concentration of bFGF and (GAGAGS) <sub>6</sub> -bFGF on proliferation of NIH- 3T3 .....	50



3.12. SF hydrogel assembly with optimal concentration of bFGF and (GAGAGS) <sub>6</sub> - bFGF formation .....	51
3.13 <i>In vitro</i> bFGF release .....	51
CHARTER IV RESULTS.....	53
4.1. Construction of (GAGAGS) <sub>n</sub> -tagged GFP expression plasmids .....	53
4.2 (GAGAGS) <sub>n</sub> tagged GFP protein expression and purification .....	63
4.3 Formation of SF/(GAGAGS) <sub>n</sub> -GFP hydrogel .....	65
4.4. <i>In vitro</i> release of GFP from SF hydrogel .....	67
4.5 <i>In vitro</i> enzymatic degradation of SF/(GAGAGS) <sub>n</sub> -GFP hydrogel .....	68
4.6 Characterization of SF/(GAGAGS) <sub>n</sub> -GFP lyophilized hydrogel .....	70
4.7 Construction of (GAGAGS) <sub>n</sub> -tagged bFGF expression plasmids .....	72
4.8 bFGF, H <sub>6</sub> -TEV-bFGF and H <sub>6</sub> -TEV-(GAGAGS) <sub>6</sub> -bFGF expression and purification....	78
4.8.1 bFGF expression and purification .....	78
4.8.2 H <sub>6</sub> -TEV-bFGF and H <sub>6</sub> -TEV-(GAGAGS) <sub>6</sub> -bFGF expression .....	82
4.9. Application of bFGF, bFGF from pMALc5x and (GAGAGS) <sub>6</sub> -bFGF peptide on tissue engineering .....	87
4.9.1 Optimization of bFGF, bFGF from pMALc5x and (GAGAGS) <sub>6</sub> -bFGF concentration for cell proliferation. ....	87
4.9.2 <i>In vitro</i> bFGF release determined by cell proliferation. ....	88
CHARPTER V DISCUSSION AND CONCLUSION .....	90
APPENDIX.....	97
REFERENCES .....	113
VITA.....	122

## LIST OF TABLES

	Page
Table 1: Synthetic polymer in therapeutic protein drugs delivery system.....	12
Table 2: Natural polymer in therapeutic protein drugs delivery system.....	13
Table 3: Silk fiber components.....	15
Table 4: Amino acid component in H-fibroin and L-fibroin of silk fibroin.....	17
Table 5: The SF biomaterial format for control drug release system.....	20
Table 6: Biodegradable polymers used for tissue engineering of cell scaffold and biosignaling molecules release.....	29
Table 7: Nucleic acid sequence of TEV-(GAGAGS) <sub>n</sub> -GFP fragment after sequencing analysis.....	55
Table 8: Amino acid sequence of recombinant peptides .....	60
Table 9: Concentration of (GAGAGS) <sub>n</sub> -GFP peptide by Bradford assay .....	64
Table 10: The gelation time point of SF solution with (GAGAGS) <sub>n</sub> -GFP peptides formed hydrogel.....	66
Table 11: DNA sequence of bFGF, TEV-bFGF, and TEV-(GAGAGS) <sub>6</sub> -bFGF fragment.....	75
Table 12: Amino acid sequence of bFGF, TEV-bFGF and TEV-(GAGAGS) <sub>6</sub> -bFGF peptides.....	77
Table 13: The concentration of bFGF recombinant peptide.....	87

## LIST OF FIGURES

	Page
Figure 1: Illustration concept of control bioactive release of SF mimetic peptide from SF hydrogel. ....	10
Figure 2: SF structure illustration including heavy chain and light chain .....	16
Figure 3: Burst release effect of bioactive molecule from SF hydrogel matrix.....	25
Figure 4: Growth factor release from biomaterial at target site in tissue engineering with uncontrol release and control release profile .....	30
Figure 5: TEV-(GAGAGS) <sub>n</sub> -GFP PCR product in 1% agarose gel. ....	54
Figure 6: SDS-PAGE of purified recombinant (GAGAGS) <sub>n</sub> -GFP peptide (a) and purified recombinant (GAGAGS) <sub>n</sub> -GFP peptide (b).....	64
Figure 7: The gelation time of SF hydrogel in different of (GAGAGS) <sub>n</sub> -GFP peptides..	66
Figure 8: In vitro release profiles of the recombinant GFP from the SF hydrogels.....	68
Figure 9: SF hydrogel degradation profile was showed the percentage of SF/(GAGAGS) <sub>n</sub> -GFP hydrogels weight remaining that incubated in protease XIV.....	69
Figure 10: Fourier-transform infrared spectroscopy (FTIR) spectra of SF hydrogel around the absorption bands of amide I and amide II.....	71
Figure 11: X-ray diffraction (XRD) pattern from 5° – 40° of SF hydrogel .....	72
Figure 12: TEV-bFGF in lane A and bfgf in lane B PCR product in 1% agarose gel.....	73
Figure 13: The optimization of IPTG varying on IPTG concentration. ....	78
Figure 14: The PEI precipitate purification in 0.25% v/v concentration.....	79
Figure 15: The purification of bFGF peptide by hydrophobic column.....	80
Figure 16: The bFGF purification by ion-exchange chromatography.....	81
Figure 17: The optimization of IPTG varying on IPTG concentration. ....	82

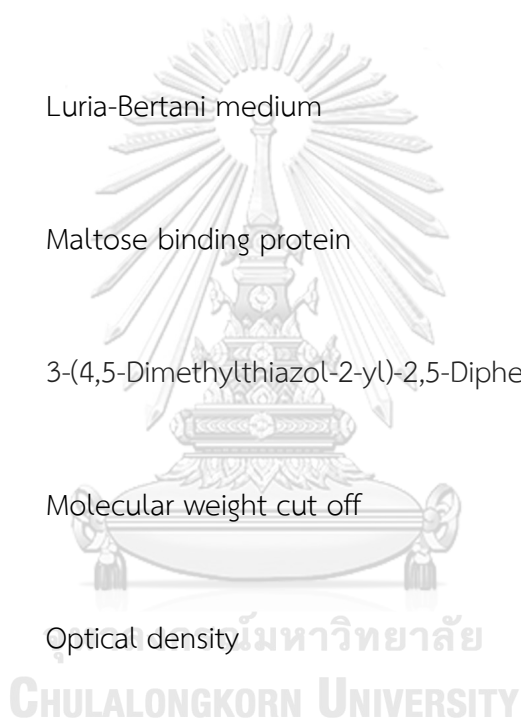
Figure 18: The histidine tag-containing TEV-bFGF purification. ....	83
Figure 19: The bFGF purification by ion-exchange chromatography. ....	84
Figure 20: The histidine tag-containing TEV-(GAGAGS) <sub>6</sub> -bFGF purification. ....	85
Figure 21: The (GAGAGS) <sub>6</sub> -bFGF purification by ion-exchange chromatography. ....	86
Figure 22: Concentration optimization of three types bFGF peptide on NIH-3T3 proliferation detected by MTT assay. ....	88
Figure 23: In vitro of bFGF release from SF hydrogel on NIH-3T3 proliferation detected by cellular activity assay (MTT). ....	89
Figure 24: Standard curve for (GAGAGS) <sub>n</sub> -GFP .....	110



## LIST OF ABBREVIATION

A	Alanine
$A_x$	Absorbance at x nm
bFGF	Basic fibroblast growth factor
CMP	Collagen mimic peptide
CRS	Control drug release system
DDS	Drug delivery system
DMEM	Dulbecco's modified engle medium
DTT	Dithiothreitol
FBS	Fetal bovine serum
FPLC	Fast protein liquid chromatography
FTIR	Fourier transforms infrared spectroscopy
G	Glycine

GFs	Growth factor
GFP	Green fluorescent protein
HEPES	4-(2-hydroxyethyl)-1-piperazineethanesulfonic acid
IPTG	Isopropyl $\beta$ -D-1-thiogalactopyranoside
LB medium	Luria-Bertani medium
MBP	Maltose binding protein
MTT	3-(4,5-Dimethylthiazol-2-yl)-2,5-Diphenyltetrazolium Bromide
MWCO	Molecular weight cut off
OD	Optical density
PBS	Phosphate-buffer saline
PEI	Poly(ethyleneimine)
PMSF	Phenylmethylsulfonyl fluoride
S	Serine



SDS-PAGE	Sodium dodecyl sulfate polyacrylamide gel electrophoresis
SF	Silk fibroin
SOC	Super optimal broth with catabolite repression
TAE	Tris-acetate-EDTA buffer
<i>Taq</i>	<i>Thermus aquaticus</i>
TEV	Tobacco etch virus
Tris	Tris-EDTA buffer
U	Enzyme unit
UP	Ultra-purified water
UV	Ultraviolet
XRD	X-ray diffraction

## CHAPTER I

### INTRODUCTION

#### 1.1 Rationales and Theories

Generally in the treatment of patients, drugs are usually applied at a fixed concentration and, ideally, the drug is released in a controlled and sustained manner. In reality, drug delivery is hardly controlled because drug release rate, drugs and tissue interaction, and drug stability are difficult to handle. To solve these limitations, drug delivery system (DDS) designed to increase the efficiency of the release and maintain the proper concentration (Tibbitt et al., 2016). There are many classes of DDS. One of them is the controlled drug release system (CRS) which is engineered to deliver drugs for days to years with a predetermined release profile (Tibbitt et al., 2016). An ideal CRS has several advantages. For example, it should maintain drug concentration within the therapeutic window. A CRS should seek to improve adherence by decreasing the number of required doses that reduce the total amount of drug needed for the therapeutic effect. Finally, the CRS should be



able to deliver a drug that rapidly degraded when administered on its own. CRS production is challenging because it requires a vehicle that can house a sufficient quantity of therapeutic, protect the therapeutic molecule, and has a predictably release lifetime (Mehtani et al., 2019).

Material production as a vehicle for carrying therapeutic has been studied in synthetic polymer, chemistry, material science, medical chemistry, and conjugated chemistry, and engineered to control the release using different material strategies (Sung & Kim, 2020). For example, in a matrix-based system, the drug diffuses through a network of interconnected pores. In a reservoir, the drug passes through a membrane. In degradable DDS, the drug is released when the materials degrade throughout. Finally, hydrogel-based DDS release drug through a constrained network whose mesh size depends on hydration and polymer architecture (Tibbitt et al., 2016). In the 1960s, the silicone tubes are designed for the hydrophobic lipophilic small molecules diffuse through the device over days to months. This device exhibited controlled compound release in the body and led to the development of the improved CRS (Hoffman, 2008). Nowadays, polymer systems for CRS have been

extensively studied as provide the ability for prolonged delivery, low toxicity, and are easy to manipulate and administer. In particular, synthetic polymers that are biodegradable polymer is preferred for use as a vehicle in CRS because they can preserve their properties for some time before they slowly dissolved into non-toxic products that can be excreted from the body. For example, poly(ethylene-co-vinyl acetate) were solubilized and mixed with lyophilized therapeutic protein and was used to release therapeutic protein at desire concentration and targeting (Akl et al., 2018). Another synthetic polymer is PEGA microspheres. This polymer is used as the vehicle for carrying and releasing prostate cancer and endometriosis drugs (Freiberg & Zhu, 2004). However, a synthetic polymer that are used as drug carriers are often synthesized using organic solvents, resulting in remaining toxic residues that limits its biocompatibility (Hamid Akash et al., 2015). On the other hand, natural polymers can be alternative for drug carriers because they can process in milder conditions. For example, Albumin can be used as a natural polymer vehicle because of its good water-solubility, readily availability, biodegradability, lack of toxicity, minimal immunogenicity, and preferential accumulation in tumor and inflamed tissues

(Elzoghby et al., 2012). It can carry drugs through two main mechanisms: albumin-drug conjugation such as a methotrexate-albumin conjugate (MTX-HAS) and drug encapsulation into albumin nanoparticles such as Abraxane. Moreover, collagen can be a carrier in the drug delivery system (Panduranga Rao, 1996). For example, there have been reported on sustained-release preparations for antibiotics such as gentamycin using collagen as a carrier. Chitosan-based drug delivery system has the potential for use as material in CRS such as chitosan-O-isopropyl-5-O-d4T monophosphate was synthesized for the treatment of HIV infection (Hu et al., 2013). However, most natural biopolymers are hydrophilic and are rapidly degraded in an aqueous environment, resulting in short drug release periods (Hamid Akash et al., 2015).

The hydrophobic natural biopolymer can alternatively be used to extend the drug release time. Especially, fibroin protein is a hydrophobic natural biopolymer suitable for controlled drug delivery because it has amphipathic and tunable properties (Kim et al., 2014). Silk fibroin (SF) is an insoluble protein with a bulky hydrophobic domain secreted by silkworm *Bombyx mori* and can be easily purified.

SF has been used as a scaffolding material because of its highly adaptable properties, excellent biocompatibility, and mild foreign body response *in vivo*. Moreover, SF can self-assemble into mechanically robust materials that are also biodegradable and non-cytotoxic. In the past decades, SF has been widely investigated in biomedical and pharmaceutical fields because of its remarkable mechanical properties, good biocompatibility, controllable biodegradability, and low immunogenicity (Altman et al., 2003). For example, SF modified chitosan nanoparticle (SF-CSNP) has been widely used as a potential drug delivery system for the treatment of hepatic cancer and achieved improved cell response (Yang et al., 2015). In addition, SF has been widely used as a tissue engineering scaffold for the generation of blood vessels, skin, bone, ligaments, and nerve (Zhang et al., 2018).

SF, the main structural protein of silk, contains polypeptide chains with molecular weight in the range of 200-350 kDa. The primary structure of SF composes of repetitive blocks of hydrophobic heavy (H) chains and hydrophilic light (L) chains. The linkers between these chains are disulfide bonds. Hydrophilic L-fibroin comprises a small number of amino acid sequences: 14% of Alanine (A), 10% of Serine (S), and

9% of Glycine (G), while hydrophobic H-fibroin consists of 46% of Glycine (G), 30.0% of Alanine (A), 12.1% Serine (S), 5.3% of Tyrosine (Y), and 1.8% of Valine (V).

Hydrophobic H-fibroin chains consist of repetitive hydrophobic domains interspersed between non-repetitive hydrophilic domains. The amino acid of repetitive

hydrophobic domains of H-fibroin fold and bond together via hydrogen bonds, Van der Waals forces, and hydrophobic interactions to form an anti-parallel  $\beta$ -sheet

crystalline structure. These crystalline domains are highly organized at the micro-level and act as crosslinking points in the less ordered, poorly oriented amorphous

matrix, which comprises random coils,  $\beta$ -turns, and  $\alpha$ -helix structures and is formed of non-repetitive domains. The strong  $\beta$ -sheet interactions, high degree of order, and

high fibroin network and thus, confer excellent mechanical strength to the silk network. The conformation and crystallinity of SF can be adjusted to control its

mechanical properties and degradation rate to make the silk fibroin control release system (Qi et al., 2017). However, the conventional SF hydrogel does not process a

linear and prolonged drug release profile. For example, SF hydrogel release diclofenac sodium into PBS buffer in a nonlinear manner with a short effective

lifetime. Hence in these systems, drugs are allowed to be released by both diffusion and degradation mechanisms, resulting in a fluctuated release profile (de Moraes et al., 2015).

One approach to achieve an extended-release profile is to tag the drug with SF-derived peptide that can interact with the SF hydrogel to reduce drug diffusion. Many researchers have tried to synthesize protein repeating units that mimic the known amino acid sequence in natural protein. For example, Collagen mimetic peptide or CMPs that mimic the natural collagen has synthesized (Gly-X-Y)<sub>7</sub>-tagged growth factor. CMPs can bind strongly to natural collagen in wound tissue and providing the option of a long-term attachment or its sustained release over a while. So, the CMPs-tagged effector molecule has an advantage for delivery of therapeutic small molecules, peptides, and proteins, and could be useful for wound healing in burn patients or slow-healing wounds in diabetic patients (Chattopadhyay et al., 2012).

The recombinant spider silk protein eADF4 (C16) is an engineered protein that mimics the known amino acid sequence of the natural silk protein eAD4 from the European garden spider *Araneus diadematus*. It comprises of 16 repeats of the amino acid

sequences: GSSAAAAAAAAAGPGGYGPENQGPSGPGGYGPGGP. These recombinant spider silk proteins can be prepared into various forms and it has been shown that spider silk is a potential candidate for a sustained drug delivery system (Spiess et al., 2010). For example, the fusion protein GFP-eADF(C16) could self-assemble into a hydrogel form and it retains the fluorescent property of GFP. From this report, it can be implied that mimicking the amino acid sequences of natural spider silk to engineer the recombinant spider silk protein could lead to an advance in CRS (Humenik et al., 2018). Similar to spider silk, the primary structure of H-fibroin of silk has highly repetitive amino acid units (GAGAGS)<sub>n</sub> that lead to the formation of secondary structure  $\beta$ -sheet. However, the development of SF repeating units as a CRS has not yet been studied before.

## 1.2 Objective of this dissertation

- To engineer SF repeating unit(s) coupled to other specific protein, green fluorescent protein (GFP), as a drug release model.

- To investigate the effect of SF repeating unit(s) on gelation of SF hydrogel and release profile of GFP model drug from SF hydrogel by degradation mechanism.
- To characterize the structure of SF hydrogel in complex with recombinant SF-tagged GFP and apply this modified SF hydrogel as a sustained drug release carriers.

### 1.3 Expected beneficial outcome from the dissertation

The SF hydrogel assembled with SF repeating unit(s) fused to bioactive molecules such as growth factors is applied and used in control drug release systems.



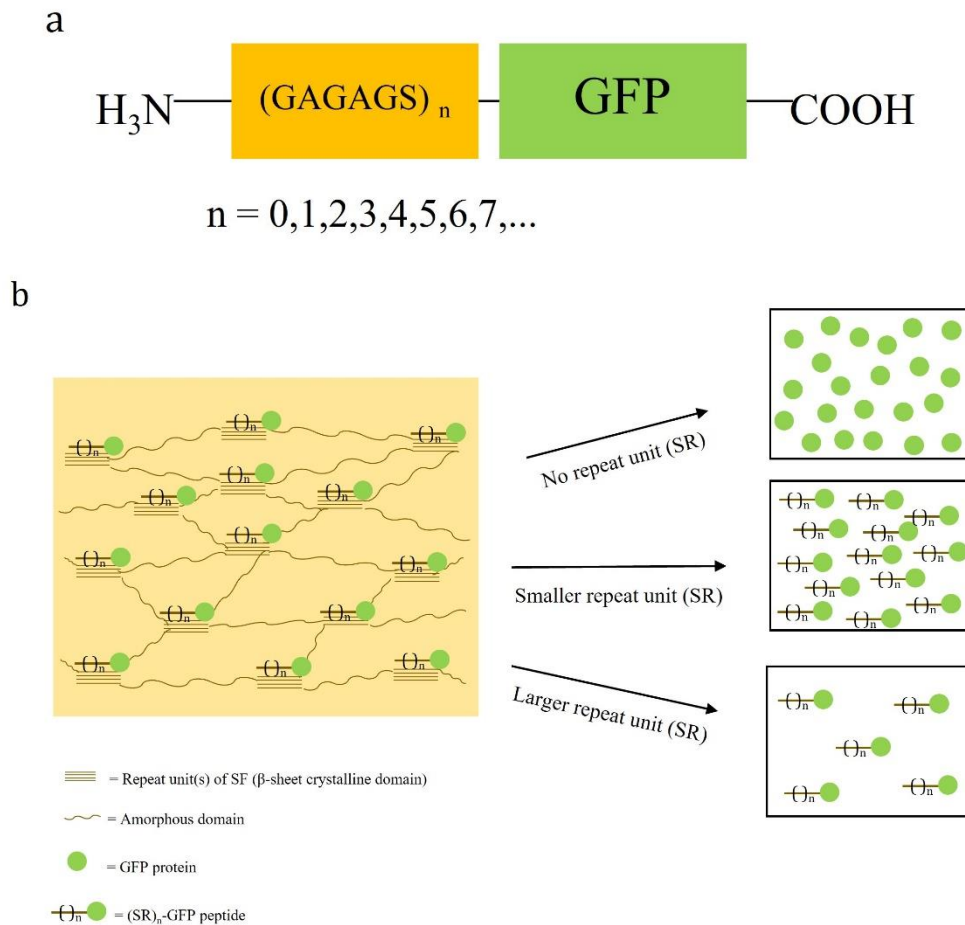


Figure 1: Illustration concept of control bioactive release of SF mimetic peptide from SF hydrogel.

- a). schematics of the SF mimetic peptide tagged bioactive molecule. b). illustration of possible interaction between the SF mimic peptide and repeats unit of SF hydrogel in control release.

## CHARTER II

### LITERATURE

#### 2.1 Control drug release system

Control drug release system (CRS) is the one important class of drug delivery system (DDS) that improved drug delivery, drug bioavailability, retain effective of drug concentration, and eliminate side effect when compared with traditional medicine. CRS production is carefully designed to allow the adequate incorporate therapeutics, protect the therapeutic damage *in vivo*, maintain activity, control release the therapeutic throughout the period, and biocompatible and degrade with non-toxic product (Tibbitt et al., 2016). Recently, the therapeutic protein is widely used in pharmaceutical and medical treatment but protein drug is rapidly digested before reaching the target site. To overcome this limitation, many materials production for CRS is designed in terms of polymers that are suitable for protecting therapeutic proteins from such extreme conditions. Many of synthetic polymers have been

intensively used for efficient delivery of protein and peptide drugs (Table 1), but protein drug is rapidly digested before target site (Fenton et al., 2018).

**Table 1: Synthetic polymer in therapeutic protein drugs delivery system.**

Synthetic Polymer	Function
PEG	PEGylation is PEG conjugated with therapeutic protein. This polymer prevents enzymatic degradation and protein immunogenicity, prolonging in body and improving the stability, and maintain pharmacokinetics and therapeutic activity.
PLGA	PLGA is biodegraded by hydrolysis of the ester linkage into non-toxic small molecule monomers and caused a non-linear and dose-dependent profile. In addition, PLGA can be copolymerizing with other polymer for improve the efficiency delivery of therapeutic protein and peptides.
PNiPAAM	PNiPAAM has a great potential for delivery of therapeutic protein and peptides but this polymer is limited because it is non-biodegradable and activated the platelets in blood.
PF127	PF127 is made up from PEO and PPO polymer. PF127 is the biomaterial for delivery of therapeutic protein, and it has shown to be non-irritant and cytocompatibility with various cell type

However, a synthetic polymer that is used as drug carriers is often synthesized using organic solvents, resulting in remaining toxic residues that limit its

biocompatibility. On the other hand, natural polymers can be alternative for drug carriers because they can be processed in milder conditions (Table 2).

**Table 2: Natural polymer in therapeutic protein drugs delivery system.**

Natural Polymer	Function
Chitosan	Chitosan is composed of D-glucosamine and acetyl-D-glucosamine that contain amino and hydroxyl group for functionalization. Chitosan is known to promote the absorption of large molecular weight therapeutic protein through intestinal epithelial mucosa. For example, chitosan has been used to enhance the absorption of insulin. Therefore, this system can be used for drug delivery.
Alginate	Alginate has been used as a component of carrier system for efficient delivery of therapeutic protein. Alginate alone or with other copolymer have been used encapsulation of therapeutic protein. This high degree of flexibility of alginate help deliver the therapeutic protein over a period ranging from minutes to months.
Gelatin	Gelatin is a protein-natured biopolymer that has thermoreversible properties. Gelatin allows easy modification on the amino acid level and also biocompatible and biodegradable. The thermogelation behavior of gelatin was improved close to body temperature by combining gelatin with therapeutic proteins. Due to its versatile characteristics, it is widely used for delivery of therapeutic molecules via targeted drug delivery system.  Collagen is the most abundant protein in the living organism. Collagen has been efficient result in sustained release of human

Collagen	growth hormone (hGH) resulting in better wound healing with a single administration of hGH
----------	--------------------------------------------------------------------------------------------

However, most natural biopolymers are hydrophilic and are rapidly degraded in an aqueous environment, resulting in a short drug release period.

## 2.2 Natural polymer-based CRS

### 2.2.1 Silk

Silk is the natural polymer or biopolymer produced from insects in arthropod phylum such as silkworms, spiders, bees. Silk is a popular material for use in medication processes like tissue engineering and drug delivery system. These silks that are used for a biomaterial in medical application is mulberry silkworms “*Bombyx mori*” (Porter & Vollrath, 2009)

Silk fiber from silkworm “*B. mori*” is the protein-polymer that is synthesized from two glands and keep in the lumen before secretion spinning fibers. At the molecular level, natural silkworm silk comprises two majors of structural proteins are fibroin and sericin (Table 3). Fibroin is the main component of silk, while

sericin is the outer glue-like coating. Silk fibers have two SF filament coated sericin. SF filaments are assembled from 3-5 nm in diameter of nanofibrils. These nanofibrils interact strongly with each other and assemble into larger fibrils are 20-200 nm in diameter to form microfibrils. The strong friction between the nanofibrils is the main reason for the strong interaction and cause the excellent mechanical strength of silk fiber.

*Table 3: Silk fiber components*

Components	Percentage (%)	Reference
Fibroin	72-81	(Inoue et al., 2000)
Sericin	19-28	
Fat/wax	0.8-1	
Color/ash	1-1.4	
Summary	100	

Silk fibroin (SF) is the hydrophobic protein and major structure of silk. SF provides mechanical strength, environmental stability, biocompatibility, and morphologic flexibility. SF contains polypeptide chains with a molecular weight of around 200-350 kDa. The primary structure of SF composes of a repetitive block of hydrophobic heavy chains (H-fibroin) and hydrophilic light chains (L-chain). The

linkers between these chains are disulfide bonds. The structure of SF protein was shown in Fig 1. In addition, glycoprotein P25 is present in the structure of SF that provides non-covalently linked to the H and L chains. The molecular ratio of H-fibroin, L-fibroin, and P25 is 6:6:1. The amino acid sequence of hydrophilic L-fibroin comprises a small number of amino acid sequences, while hydrophobic H-fibroin has many amino acid sequences that show in table 4.

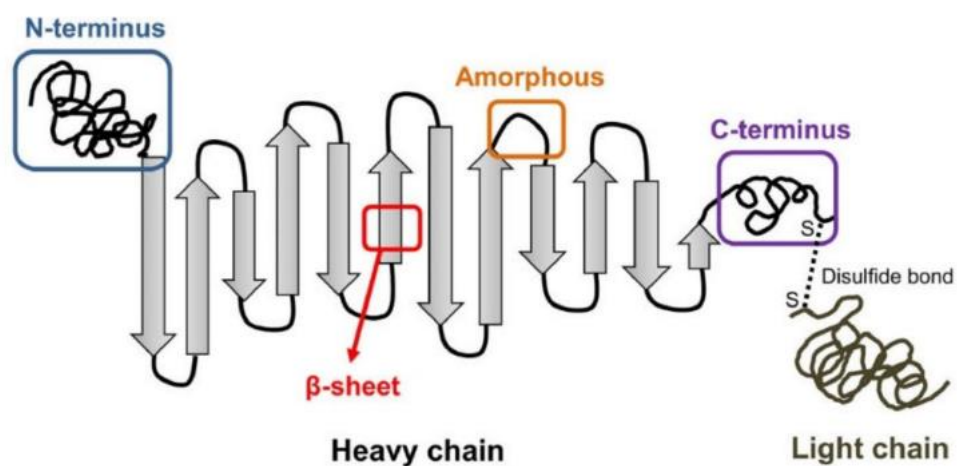


Figure 2: SF structure illustration including heavy chain and light chain (Zuluaga-Vélez et al., 2019).

*Table 4: Amino acid component in H-fibroin and L-fibroin of silk fibroin.*

Amino acids	mol% of amino acid residues	
	H-chain	Light-chain
Glycine	49.4	10.0
Alanine	29.8	16.9
Serine	29.8	7.9
Tyrosine	4.6	3.4
Valine	2.0	7.4
Aspartic acid	0.65	15.4
Glutamic acid	0.70	8.4
Threonine	0.45	2.8
Phenylalanine	0.39	2.7
Methionine	-	0.37
Isoleucine	0.14	7.3
Leucine	0.09	7.2
Proline	0.31	3.0
Arginine	0.18	3.8
Histidine	0.09	1.6
Lysine	0.06	1.5

From the amino acid sequence in H-fibroin, the amino acid sequence is a repeat unit block and can be described as (-Gly-Ala-Gly-Ala-Gly-Ser-)<sub>n</sub>. The repetitive hydrophobic amino acid domains of H-fibroin fold and bond together via hydrogen bonds, Van der Waals forces, and hydrophobic interaction, to form an anti-parallel  $\beta$ -sheet crystalline structure. These crystalline domains are highly organized at a microscopic level and act as crosslinking points in the less ordered, poorly oriented



amorphous matrix, which comprise random coils,  $\beta$ -turns, and/or  $\alpha$ -helix structures and is formed of a non-repetitive domain that causes to finish of structure organization. The secondary structures of silk could be classified into three crystalline forms: silk I, silk II, and silk III. Silk I is a liquid state that is a metastable form of SF stored in the gland of silkworms and the major structure contains  $\alpha$ -helix and even random coil secondary structure. Conversely, silk II is a solid-state that forms after spinning and has a  $\beta$ -sheet crystalline secondary structure. Lastly, silk III is a solid form of SF that has trifold helical chain conformation and is found at the air/water interface. During silkworm spinning, the conformation of silk changes from a dissolved solution of silk I to the solid form of silk II that are highly ordered structure to form of silk fibers (Nguyen et al., 2019). To investigate the secondary of SF protein, Fourier transforms Infrared Spectrophotometry (FTIR) was used to identify the structure of SF. The SF structure revealed two different structure models: silk I is known to be rich in  $\alpha$ -helical structure occur at 1650-1658, 1545, and 1240  $\text{cm}^{-1}$  respectively; silk II of SF structure is known to be rich in  $\beta$ -sheet and had infrared absorption peaks in the amide I, II and III at 1625-1640, 1515-1525, and 1240  $\text{cm}^{-1}$  respectively; and those

of random coils occur at 1640-1648, 1535-1545 and 1235  $\text{cm}^{-1}$  respectively. In addition, X-ray diffraction (XRD) is the other method for characterized the structure of SF in terms of the crystalline region in SF structure. XRD pattern peak of SF protein appears at 12.2°, 19.7°, 24.7°, and 28.2° for silk I and at 9.1°, 18.9°, and 20.7° for silk II (Wang & Zhang, 2013).

### 2.2.2 Silk fibroin for control drug delivery system

From the amphipathic structure of SF, the crystalline domain in SF provides excellent properties such as control drug release and degradation profile. There are various research to used SF as a biomaterial for control drug release (Tomeh et al., 2019). There has been much research to produce the SF biomaterial in various format for control and sustain drug or therapeutic agent release that showed in table

5.

*Table 5: The SF biomaterial format for control drug release system.*

Formulation	Therapeutic/drug	Outcome	Ref.
Disk	HIV inhibitors	Disk format of SF can stabilize microbial contamination during storage. SF disk can deliver in local route and sustained HIV inhibitor over 4 weeks.	(Zhang et al., 2017)
Films	Theophyllin	This format can used in transdermal delivery and sustained release up to a week.	(Rujiravanit et al., 2003)
	Diclofenac Sodium	SF films can cross-link with chitosan and control release over 10 days	
	Amoxicillin	SF films can be designed for pH-dependent release (pH2 > pH 5.5 > pH 7.2) over 10 hours.	
	Nerve growth factor (NGF)	Designed to be used as a nerve conduit in peripheral nerve defect. NGF release for over 3 week and conduct PC12 cells proliferation and maturation.	(Uebersax et al., 2007)
Coating	Rhodamine B	Sustained release up to 40 days with layer-by-layer silk coating	(Wang et al., 2007)
	Heparin	Multi-layer silk coating for vascular stent	(Wang et al., 2008)
	Epirubicin Hydrochloride	Layer-by-layer heparin-silk nanofilms. This system can control epirubicin hydrochloride drug release up to 7 days.	(Choi et al., 2018)
	Theophyllin	Silk used as the film coating material on a drug tablet. Drug release was sustained following zero order kinetics	(Bayraktar et al., 2005)
Forms	Vincristine	Silk forms can use in intratumoral implantation that decreased tumor growth	(J. M. Coburn et al., 2017)

		by sustained release up to 48 days.	
Microneedles	Tetracycline	This format is mild drug encapsulation method and has activity of 10-fold reduction in bacterial density.	(Tsioris et al., 2012)
	Vaccination against: Influenza	Vaccine coated on silk microneedles and showed in vivo immune response over 28 days.	(Stinson et al., 2017)
Reservoirs	Anastrozole	Silk rod reservoirs can used as implant systems for cancer therapy. This system showed sustain release up to 91 days following zero order kinetics.	(Yucel et al., 2014)
	Cisplatin	Cisplatin release over 30 days from silk reservoirs. This format can allow high drug loading and can used in intratumoral application.	(Yavuz et al., 2019)

### 2.2.3 Silk fibroin hydrogel for control drug release

Hydrogels are three-dimension (3D) macromolecular polymeric chains that can be easily molded in any form, shape, and size. There is a particularly appealing type of drug delivery system and has been used in many-branched of medicine, including tissue engineering, cardiology, oncology, immunology, wound healing, and pain management. Generally, hydrogels are composed of a large amount of water and a cross-linked polymer network. The high water content provides physical

similarity to tissue and can give the hydrogel excellent biocompatibility and easily encapsulate hydrophilic drug (Galateanu et al., 2019).

Silk materials can be fabricated into various formats such as films, particles, and gel. Interestingly, hydrogel format has specifically aqueous-based platforms as their properties lend unity for a diversity of medical applications. Hydrogel-based silks have been thoroughly studied for potential biomedical applications due to their mechanical properties, biocompatibility, controllable degradation rates, and self-assembly into  $\beta$ -sheet networks.

Normally, SF hydrogel is an excellent choice for the delivery of small drug molecules that is stabilized drug efficiency. Typically, after incorporating them into the SF network, therapeutic agents are maintained, transported to the target sites, and released in a controlled manner. For example, SF hydrogel incorporated with an antibiotic such as penicillin, ampicillin, cefazolin, rifampicin, erythromycin, and tetracycline demonstrated rapidly release in 1-5 days, but SF hydrogel preserved antibody efficacy through *in vivo* and *in vitro* bacterial growth (Pritchard et al., 2013).

Fang et al. investigated the rapid release of buprenorphine from SF hydrogel via hydrogel mesh size and SF concentration (Fang et al., 2006). In addition, Seib et al. used an SF-based hydrogel to deliver doxorubicin (DOX) for the localized treatment of primary breast cancer. The SF-DOX hydrogel could be normally released from hydrogel and exhibit highly tumor regression response and reduced metastatic spread (J. Coburn et al., 2017). In addition, not only the delivery of small molecule drugs but also the delivery of biological molecules such as proteins, growth factors, peptides, and gene is also an important area of biomedical application. For example, In 2011 reported monoclonal antibody that could be released and maintained from SF hydrogel over an extended period by the high density of the crystalline network of hydrogel (Guziewicz et al., 2011). Uebersax et al. used SF-base hydrogel blended with nerve growth factor (NGF) for control release of growth factor in tissue engineering. Afterward, it was demonstrated that the proliferation and differentiation of PC12 cells that caused by sustained release of NGF from hydrogel (Uebersax et al., 2007) but this process occurs rapidly bioactive release in uncontrolled fashion as shown in Fig 2. To improve these limitation, SF-based hydrogel mixed with other

polymeric molecules was used in control bioactive release to improve release efficacy. For example, SF/polyacrylamide (PAAm) is an example of an SF-based protein delivery system for the delivery of FITC-labelled insulin (Mandal et al., 2009). The release profile of insulin of this hydrogel was controlled and sustained release by increasing additional polymer. In addition, the vascular endothelial growth factor (VEGF) was used as a cytokine model and was non-covalently encapsulated into composite gels before crosslinking it in the presence of polyethylene glycol diacrylate. The additional of 0.3% thiol-modified heparin to the release medium led to the increase in the present release of VEGF from 25% to 75% over 42 days (Elia et al., 2013). In 2015, composite hydrogels were prepared by blending SF with the copolymer. Aspirin and indomethacin were incorporated into SF/copolymer hydrogels as two model drugs with different water solubility. The hydrophilic and hydrophobic drug release was showed differently release profiles upon different of interaction between drug and copolymer (Zhong et al., 2015).

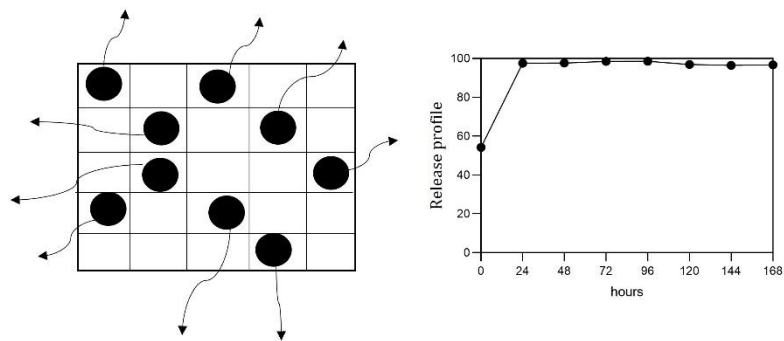


Figure 3: Burst release effect of bioactive molecule from SF hydrogel matrix

### 2.3 Biomimetic peptide for control drug release

Biomimetic peptides are synthetic compounds that are identical to amino acid sequences synthesized by chemical or biological processes (Vincent, 2014). For example, Collagen mimetic peptide or CMPs that mimic the natural collagen has synthesized (Gly-X-Y)<sub>7</sub>-tagged growth factor. CMPs can bind strongly to natural collagen in wound tissue and providing the option of a long-term attachment or its sustained release over a while. So, the CMPs-tagged effector molecule has an advantage for delivery of therapeutic small molecules, peptides, and proteins, and could be useful for wound healing in burn patients or slow-healing wounds in diabetic patients (Chattopadhyay et al., 2012). In the case of silk, much research was on synthesized recombinant spider silk mimic peptides because it is particularly



difficult to domesticate. Most recombinant spider silk proteins are based on *Nephila clavipes* refer to their spidroins as MaSp1 and MaSp2 depending on proline amino acid content. This recombinant was showed delivery of DNA plasmid to a tumor target site (Numata et al., 2012). Moreover, the recombinant spider silk protein eADF4 (C16) is an engineered protein that mimics the know amino acid sequence of the natural silk protein eAD4 from European garden spider *Araneus diadematus*. It comprises of 16 repeats of the amino acid sequences: GSSAAAAAAGPGGYGPENQGPSGGYGPGGP. These recombinant spider silk proteins can be prepared into various forms, and it has been shown that spider silk is a potential candidate for a sustained drug delivery system. (Lammel et al., 2011). In addition, the fusion protein GFP-eADF(C16) could self-assemble into a hydrogel form and it retains the fluorescent property of GFP. From this report, it can be implied that mimicking the amino acid sequences of natural spider silk to engineer the recombinant spider silk protein could lead to an advance in the drug delivery system (Humenik et al., 2018).

Accordingly, the structure in SF of silk from *Bombyx mori* that has a repeating block in a hydrophobic domain can control its mechanical properties and degradation rate to make the SF control release system. For example, Silk-elastin-like protein polymers (SELPs) are block copolymers consisting of an amino acid repeat (GAGAGS) of SF from *B. mori* silk and mammalian elastin (GVGVP). SELPs have been examined for controlled release of markers and bioactive agents from low molecular weight to high molecular weight controlling by a concentration of polymer and development of structure of this polymer (Dinerman et al., 2002). In addition, Gene delivery from SELPs has also been explored by examining the character of DNA plasmid release but the route of gene transfer often lacks the efficiency (Megeed et al., 2002).



#### **2.4 Control release of biosignalling on tissue engineering application**

Tissue engineering is a new area of biomedical technology and methodology to assist and accelerate the regeneration of damaged tissue based on the natural healing of patients themselves. Biomaterial technology plays an important role in the creation of cell environments such as scaffold and drug delivery systems of signaling

molecules that have been investigated to enhance proliferation and differentiation of cell potential for tissue engineering.

Basically, body tissue is composed of cells, and the surrounding environment that includes extracellular matrix (ECM) for cell proliferation and differentiation as the living places of cells and signaling molecules. There is some case where tissue regeneration is involved by single or combination of cell and the environment surrounding. To the end, biomaterial plays a key role in designing and creating substitutes for ECM and the drug delivery system (DDS) of signaling molecules to enhance their biological application. As the biomaterial, various synthetic and natural materials, such as polymers, ceramics, and metals or their composites, have been investigated and used in different manners. Among them, biodegradable biomaterials are an example in table 6 (Tabata, 2003).

*Table 6: Biodegradable polymers used for tissue engineering of cell scaffold and biosignaling molecules release.*

Synthetic polymer	Natural polymer
Poly(L-lactic acid) (PLLA)	Collagen
Poly(glycolic acid) (PGA)	Gelatin
Poly( $\epsilon$ -caprolactone) (PCA)	Fibrin
Copoly(LL-GA)	Hyaluronic acid
Copoly(LLCA)	Alginate
Copoly(LLA-ethylene glycol (EG))	Chitosan
Copoly(fumarate-EG)	Chitin

Although the growth factors are playing important role in tissue regeneration, the directly inject of growth factor into site effect is not effective. The growth factors are rapidly diffused from the injected site and rapidly degrade with local enzymatic. To overcome this limitation, the growth factors are incorporated into biomaterial for control growth factor release in appropriated manner but this process still has uncontrolled release profile as shown in figure 3.

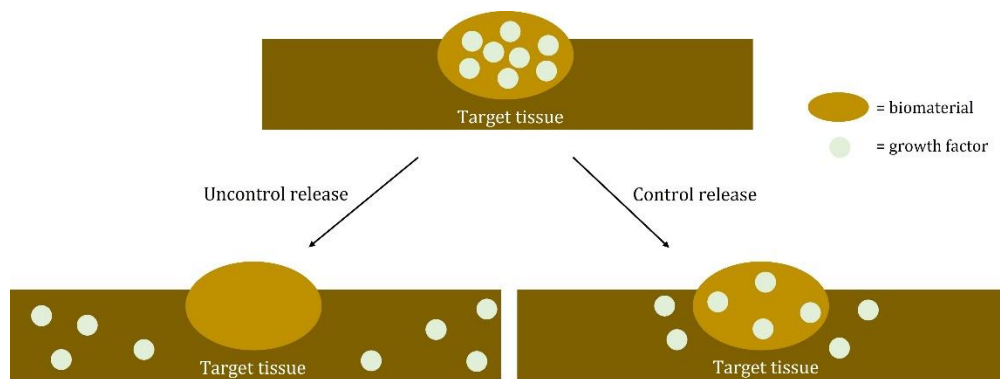


*Figure 4: Growth factor release from biomaterial at target site in tissue engineering with uncontrol release and control release profile*

#### 2.4.1 Biosinalling in tissue engineering

Growth factors (GFs) are a type of biosignaling molecule that are powerful therapeutic agents for tissue regeneration. GFs are soluble proteins secreted by cells that can regulate a wide range of cellular behaviors, such as proliferation, migration, and differentiation, by binding to specific transmembrane receptors on target cells (Tabata, 2003). Some of the widely studied GFs in tissue regeneration and repair are involved in angiogenesis and osteogenesis. These include vascular endothelial growth factors (VEGFs) (Brandi & Collin-Osdoby, 2006), fibroblast growth factor (FGF) (Martino et al., 2015), and placental growth factors (PIGFs) which are involved in angiogenesis and play a crucial role in the repair of most tissue, insulin-like growth factors (IGFs),

transforming growth factor beta (TGF- $\beta$ ), bone morphogenetic proteins (BMPs) (Kirker-Head, 2000) which are the most extensively used osteogenic proteins for inducing new bone formation in bone defects and ectopic sites.

#### 2.4.1.1 Basic fibroblast growth factor (bFGF)

Basic fibroblast growth factor (bFGF) is one type of fibroblast growth factor and shows a widely of biological activity. bFGF has 9.6 isoelectric points (pI) and was firstly identified by its ability to cause the proliferation and phenotypic transformation of NIH-3T3 fibroblast cell (Gospodarowicz, 1974). Most of the biological studies with fibroblast growth factors have been done with basic form (bFGF). bFGF has both acute and long-term effects on the morphology and growth pattern of responsive cells. Human skin fibroblasts maintained with bFGF in serum-supplemented medium become extremely elongated with slender projections. In addition, bFGF is a potent mitogen for mesoderm-derived cells. When tested on vascular endothelial cells derived from either large vessels or capillaries, it triggers cell proliferation at a concentration as low as 2 pg/ml. This concentration is 20 to 60-fold lower than those required to see comparable effects on cell growth or the

initiation of DNA synthesis with TGF $\beta$ , EGF, or PDGF. bFGF stabilizes the phenotypic expression of cultured cells. This factor has made possible the long term culturing of the cell types that otherwise would lose their normal phenotypes in culture when passaged repeatedly at a low cell density (Nugent & Iozzo, 2000).



## CHAPTER III

### METHODOLOGY

#### 3.1 Construction of (GAGAGS)<sub>n</sub>-tagged GFP expression plasmid

Green fluorescent protein (GFP) amino acid sequence was translated into DNA sequence considering bacteria codon usage. For construction of pMALc5x-TEV-GFP expression plasmid, primer A and primer H (Table 18 in appendix) were used in polymerase chain reaction (PCR) to amplify the GFP gene from pEGFP-N1. The PCR reaction recipe contained as follows: 0.5 ng/ $\mu$ L pEGFP-N1, 0.25  $\mu$ M forward primer A and reverse primer H (primer sequences are shown in table 18 in appendix), 0.2 mM dNTP, 5% v/v Dimethyl sulfoxide (DMSO), 0.02 U/ $\mu$ L Phusion hot-start polymerase, and the volume of UP water adjusted to an appropriate volume. The PCR reaction was introduced to Thermo Scientific Arktik Thermal Cycler, the PCR condition as follows: initial denaturing of 98 °C for 30 seconds; 25 cycles of 98 °C for 10 seconds, 60 °C for 30 seconds, 72 °C for 30 seconds; and one final extension cycle of 72 °C 5 minutes. The PCR product was purified by agarose gel electrophoresis. The PCR



sample was mixed with 6x Gel Loading Dye Purple (Biolab) before adding (30  $\mu\text{L}$ ) into the well of 1% agarose gel in 1x TAE buffer with Hydra Green dye. The 1 kb Gold Bio DNA marker (5  $\mu\text{L}$ ) was added in the first lane. DNA separation condition was constant voltage at 100 V for 45 minutes. After the separation had finished, the gel was visualized under the UV light and cut gel between 750 and 1000 band size and cleaned up using Bio Fact Hi gene<sup>TM</sup> gel & PCR Purification. After purifying the PCR product, The PCR product, and pMALc5x construct plasmid was cut with 5 U/ $\mu\text{L}$  NcoI and 10 U/ $\mu\text{L}$  BamHI restriction enzyme and incubated at 37 °C for 1 hour. Then, the constructed plasmid was dephosphorylated with 1 U/ $\mu\text{L}$  shrimp alkaline phosphatase (rSAP) and incubated at 37 °C for 30 minutes. The digested PCR product and pMALc5x were cleaned up with Bio Fact Hi gene<sup>TM</sup> gel & PCR Purification. The purify digested PCR product and pMALc5x were cloned using a molar ratio of 1:3 construct vector to PCR product by 80 U/ $\mu\text{L}$  T4 DNA ligase and incubated at 4 °C for 4-6 hours. The ligation solution was transformed into *E. coli* DH10 $\beta$  using heat shock method. Ligation solution (5  $\mu\text{L}$ ) was added into the 50  $\mu\text{L}$  of competent *E.*

*coli* DH10 $\beta$ , and incubated for 30 minutes on ice. The mixture was dipped into 42 °C water for 30 seconds, then the tube was set on ice for 2 minutes. The transformed cell was added to the 250  $\mu$ L of SOC, and shook at 37 °C, 250 rpm for 1 hour. Lastly, 300  $\mu$ L of the mixture was spread on LB agar plates that contain 100  $\mu$ g/ml ampicillin and incubated at 37 °C for 16 – 18 hours, and colonies occurred.

The single colony was picked into a tube of LB broth (5 ml) containing the same concentration of antibiotics and shook at 37 °C, 250 rpm overnight. PCR was then performed to confirm the successful construction *tev-gfp* gene into pMALc5x plasmid. For each reaction, cell culture (1  $\mu$ L) was added into 9  $\mu$ L of UP water, boiled the sample on 98 °C for 3 minutes. The boiled sample was used as the template for the PCR. The PCR reaction composition was as follows: 2 mM MgCl<sub>2</sub>, 0.2 mM dNTP, 0.5  $\mu$ M forward primer 1 and reverse primer 1, 0.01 U/ $\mu$ L Taq DNA polymerase, and 10  $\mu$ L boiled sample. The PCR products were analyzed by agarose gel electrophoresis. The sample was mixed with 6x Gel Loading Dye Purple (Biolab) before adding (20  $\mu$ L) into the well of 1% agarose gel in 1x TAE buffer with Hydra

Green dye. The ladder 1 kb Gold Bio DNA marker (5  $\mu$ L) was added in the first well. DNA separation condition was constant voltage at 100 V for 45 minutes. After the separation had finished, the gel was visualized under UV light. The positive clones would appear between 750 bases to 1000 bases band size. The positive colony cell culture (1.5 ml) was extracted of plasmid using the method and materials suggested in the BioFact™ Plasmid Mini Prep Kit. Finally, the positive plasmid concentration was determined by spectrophotometry at  $A_{260}$  before sequencing to confirm the correct construction plasmid.

Other expression plasmids were generated a similar manner. Briefly, for the pMALc5x-TEV-GAGAGS-GFP expression plasmid, primers B and H were used to amplify the pMALc5x-TEV-GFP template. For the pMALc5x-TEV-(GAGAGS)<sub>2</sub>-GFP expression plasmid, primers C and H were used to amplify the pMALc5x-TEV-GAGAGS-GFP template. For the pMALc5x-TEV-(GAGAGS)<sub>3</sub>-GFP expression plasmid, primers D and H were used to amplify the pEGFP-N1 template. For pMALc5x-TEV-(GAGAGS)<sub>4</sub>-GFP expression plasmid, primers E and H were used to amplify the pMALc5x-TEV-(GAGAGS)<sub>3</sub>-GFP template to obtain the TEV-(GAGAGS)<sub>4</sub>-GFP PCR product. For

pMALc5x-TEV-(GAGAGS)<sub>5</sub>-GFP, the TEV-(GAGAGS)<sub>4</sub>-GFP PCR product was re-amplified with primers F and H to obtain TEV-(GAGAGS)<sub>5</sub>-GFP for cloning. The TEV-(GAGAGS)<sub>4</sub>-GFP PCR product was also re-amplified with primers G and H to obtain the TEV-(GAGAGS)<sub>6</sub>-GFP PCR product for cloning. The nucleotide sequences of all expression plasmids were confirmed by DNA sequencing.

### 3.2 (GAGAGS)<sub>n</sub> tagged GFP protein expression and purification

The suspension of competent *E. coli* tuner (DE3) (50  $\mu$ L) was incubated on ice and 3  $\mu$ L of pMALc5x-TEV-(GAGAGS)<sub>n</sub>-GFP, 20  $\mu$ L of KCM, and 27  $\mu$ L of sterile distilled water were added. After incubation on ice for 30 minutes, the mixture was heat-shocked at 42 °C for 30 seconds, then on ice for 2 minutes. SOC media (250  $\mu$ L) was added to the mixture before shook at 37 °C for 1 hour. The cells (100  $\mu$ L) were spread on an LB agar plate containing 100  $\mu$ g/ml of ampicillin. This plate was incubated at 37 °C for 16-18 hours. *E. coli* tuner (DE3) that was transformed with pMALc5x-TEV-(GAGAGS)<sub>n</sub>-GFP has grown in 100 ml Terrific Broth with 100  $\mu$ g/ml ampicillin at 37 °C for 16 – 18 hours. Cell cultures were grown in 500 ml Terrific

Broth using 3% inoculum of starter at 37 °C until  $OD_{600}$  occurred around 0.4 – 0.6. IPTG was added to cell culture at 1 mM final concentration. The culture was incubated at 30 °C for 6 hours. Finally, the cell culture was harvested by centrifugation at 6,000 xg for 10 minutes and frozen the cell pellet at -80 °C.

The cell pellet was resuspended in 30 ml of buffer A (25 mM HEPES, 150 mM NaCl, and 25 mM Imidazole; pH 7.5). Lysozyme (10 mg/ml, 100  $\mu$ L) was added, and the mixture was incubated at room temperature for 30 minutes, then PMSF (500  $\mu$ L) was added. Then, the mixture was sonicated using BANDELIN SONOPULS HD 2200 homogenizer, KE76 probe, for 15 seconds, 30% of pulse cycle, and 40% of power and disrupted the mixture until the mixture became less viscous. The suspension was centrifuged at 40,000 xg, 4 °C for 30 minutes. The supernatant was loaded onto 3-ml Ni-NTA agarose Beads column equilibrated in buffer A. Non-specific binding protein was washed with buffer A. Elution was performed single step with buffer A changing 25 mM to 250 mM Imidazole. MBP-TEV-(GAGAGS)<sub>n</sub>-GFP was digested with TEV proteinase and 100 mM DTT at 4 °C for 24 hours or until digested completely detected by SDS-gel electrophoresis. After that, the digestive protein was dialyzed in

buffer A and purify again in Ni-NTA Agarose Beads column. The purify protein was dialyzed against 20 mM Tris, pH 7.5. The (GAGAGS)<sub>n</sub>-GFP was loaded onto 1 ml Q-Sepharose column (GE Healthcare) pre-equilibrated with buffer B (20 mM Tris, pH 7.0) and washed with buffer B (20 mM Tris 60 mM NaCl, pH 7.0) for removal TEV proteinase. The purify (GAGAGS)<sub>n</sub>-GFP peptide was eluted with buffer B (20 mM Tris 100 mM NaCl). The purity of (GAGAGS)<sub>n</sub>-GFP was checked by using SDS-PAGE and Coomassie Brilliant blue staining. The pure (GAGAGS)<sub>n</sub>-GFP peptide was dialyzed against 20 mM Tris, pH 7.0 overnight. The dialyzed protein was concentrated using centrifugal filter before determining concentration by Bradford assay.

### 3.3 Preparation of silk fibroin solution

Silk cocoon “Nangnoi Srisaket” of thai silkworm *B. mori* was cleaned to remove the outer layer of irregular fibers on the cocoons such as dirt, dead silkworm, and other visible contaminants. The clean cocoon was dissolved in 0.2 Na<sub>2</sub>CO<sub>3</sub> solution for remove sericin protein. The solution was heated until its boiling point and then cleaned silk cocoon (40 g) was added into boiling solution. The sericin was removed after 20 minutes. The silk fibers were washed with distill water until the

water appear colorless and dried at room temperature for 2 days. After that, the dried silk fibers were sterilized with steam and pressure for 15 minutes. The sterilized silk fibers (4 g) were dissolved in 9.3 M LiBr solution and placed in 60 °C oven. The amber viscous of dissolved silk fibers was occurred after 4 hours. To remove the LiBr from SF solution, the solution was dialyzed in distil water for 48 hours using dialysis bag with 12-16 MWCO. The dialysis solution was centrifuged for remove the impurities at 9,000 rpm, 4 °C for 20 minutes. Finally, the SF solution was measured concentration in percentage of weight by volume.

### 3.4 Silk fibroin gelation time detection

The SF stock solution was prepared at 4% (w/v) concentration by dilution with deionized water, and the (GAGAGS)<sub>n</sub>-GFP stock solutions were prepared to 100 µg/ml concentration. The SF stock solution (100 µl) and the (GAGAGS)<sub>n</sub>-GFP stock solution (100 µl) were mixed in a well of a 96-well plate. The solution was incubated at 37°C until the gelation occurred. The gelation kinetic was determined by tracking the absorbance of 550 nm light because SF absorbs light best at 550 nm

when gelled but barely absorbs 550 nm before gelled. Microplate reader (absorbance mode) was used to determine the sol-gel transition.

### 3.5 *In vitro* GFP release

To determine the release profile of GFP as a model drug, the SF hydrogels were collected from 96-well plate. The amount of GFP release from SF hydrogel was measured by its absorbance at 395 nm using spectrophotometer. The hydrogel was cut into cubic shape (2\*2\*2 mm) and weighed around 20 mg of each sample. The SF hydrogel was submerged in 1 ml of deionized water in cuvette. The absorbance values at 395 nm were recorded every 10 minutes within the first 2 hours, and then every 12 hours until the absorbance values no longer changed.

### 3.6 *In vitro* enzymatic degradation of silk fibroin hydrogel

The cubic sample of SF hydrogel was cut in 4 mm\*4 mm\* 4 mm and weighted around 40 mg. The sample cubic were submerged in PBS buffer (10 ml) that contained proteinase XIV (1 U/ml) and incubated at 37 °C for 30 days. The buffer solution was taken out and replaced daily by fresh buffer with enzyme. At a specific



time point, the buffer was removed. The retrieved hydrogel cube was rinsed with distilled water, and the weight of hydrogel was determined. The weight ratio was calculated as follows equation 1.

$$\% \text{ of gel weight remaining} = \frac{W_t}{W_0} \times 100 \quad (\text{Equation 1})$$

$W_0$  = Weight of SF hydrogel before added enzyme

$W_t$  = Weight of SF hydrogel remaining at every 2 days interval

### 3.7 SF hydrogel structure characterization

#### 3.7.1 Lyophilized silk fibroin assemble with (GAGAGS)<sub>n</sub>-GFP-H<sub>6</sub> peptide

##### hydrogel

Lyophilized-gel was prepared by lyophilized in a freeze dryer. The hydrogel sample was first prefrozen in liquid nitrogen for quick-frozen to avoid structural changes, then was stored at -20 °C overnight before lyophilization. The drying SF hydrogel sample was performed at -54 °C, 0.1 mbar (vacuum) for 72 hours. Finally, lyophilized-gel samples were stored at 4 °C before characterization.

### 3.7.2 X-ray diffraction (XRD) of SF lyophilized gel

The XRD analysis of the hydrogels was performed using X-ray diffractometer (Rigaku, Smartlab 30 kV) equipped with a fixed monochromator and CuK $\alpha$  radiation source. All patterns were measured at  $2\theta$  in the range of 5-40°. The diffraction at the  $2\theta$  angle of 19.5 – 22.5° is represented of the SF crystalline fraction.

### 3.7.3 Fourier-transform infrared (FTIR) spectroscopy

The lyophilized-gel samples were first placed onto IR-transparent discs and then analyzed using sn FTIR microscopic spectrometer (Nicolet iS50 FTIR, Thermo Fisher Scientific, Waltham, MA, USA). The spectrum of infrared was collected between 4000 to 400  $\text{cm}^{-1}$  in a transmission mode. The absorption of amide I is 1650  $\text{cm}^{-1}$  for the random coils and 1630  $\text{cm}^{-1}$  for  $\beta$ -sheets. The absorption of amide II is 1540  $\text{cm}^{-1}$  for the random coils and 1520  $\text{cm}^{-1}$  for the  $\beta$ -sheets.

### 3.8 Construction of (GAGAGS)<sub>n</sub>-tagged bFGF expression plasmid

For the construction of the pET28b-bFGF expression plasmid for produced the native bFGF that didn't have tag or any linker, primers I and K (table 18 in

appendix) were used in polymerase chain reaction (PCR) to amplify the GFP gene from cDNA of HeLa cells and cloned into the NcoI and HindIII sites of pET28b. The PCR reaction recipe contained as follows: 0.5 ng/ $\mu$ L GFP cDNA, 0.25  $\mu$ M forward primer1 and reverse primer1 (primer sequences are shown in the appendix), 0.2 mM dNTP, 5% v/v Dimethyl sulfoxide (DMSO), 0.02 U/ $\mu$ L Phusion hot-start polymerase, and the volume of UP water adjusted to an appropriate volume. The PCR reaction, ligation, transformation, and collected positive clones were followed as describes in methodology 3.1. For the pMALc5x-H<sub>6</sub>-TEV-bFGF expression plasmid was generated in a similar manner, primers J and K were used to amplify the cDNA of HeLa cells templated. And the pMALc5x-H<sub>6</sub>-TEV-(GAGAGS)<sub>6</sub>-bFGF expression plasmid was purchased from Biomatik.

### 3.9 bFGF and (GAGAGS)<sub>6</sub>-bFGF expression and purification

#### 3.9.1 IPTG optimization for bFGF and (GAGAGS)<sub>6</sub>-bFGF expression

The transformed *E. coli* tuner (DE3) with pET28b-bFGF was cultured in LB (containing 50  $\mu$ g/ml of kanamycin) until the OD<sub>600</sub> reached 0.6. And the transformed

cells with pMALc5x-H<sub>6</sub>-TEV-bFGF, and pMALc5x-H<sub>6</sub>-TEV-(GAGAGS)<sub>6</sub>-bFGF were cultured in LB (containing 100 µg/ml of ampicillin) until the OD<sub>600</sub> reached 0.6 too. The cultures (2 ml) were aliquoted and IPTG were added (0 – 1 mM) to induce protein expression for 4 hours. The cell pellets were collected before adding 500 µL of the detergent solution (20 mM Tris, pH 7.0, 0.5% octylthioglucoside, 5 µg of the 10 mg/ml lysozyme, and 0.25 µL of 5 U/µL benzonase) to break the cells for 15 minutes. After centrifugation, the supernatants were collected into new tube while water 500 µL were added to the remaining pellet. Loading buffer with DTT (6x) were added to the supernatant and cell debris before boiling. The protein samples were analyzed by SDS-PAGE electrophoresis.



### 3.9.2 bFGF and (GAGAGS)<sub>6</sub>-bFGF expression using *Escherichia coli* Tuner

(DE3)

The transformed cells containing pET28b-bFGF was picked into 50 ml of of kanamycin-containing terrific broth and the transformed cells with pMALc5x-H<sub>6</sub>-TEV-bFGF, and pMALc5x-H<sub>6</sub>-TEV-(GAGAGS)<sub>6</sub>-bFGF were picked into 50 ml ampicillin terrific

broth as the starter culture for large scale production then incubated at 37 °C for 16 – 18 hours. For bFGF expressed from pET28b-bFGF, four flasks of 500 ml of terrific broth containing 50 µg/ml kanamycin were inoculated with 15 ml of the starter culture. And bFGF and (GAGAGS)<sub>6</sub>-bFGF from pMALc5x plasmid production, four flasks of 500 ml ampicillin-terrific broth were inoculated with 15 ml of the culture starter. All flasks were shaken at 37 °C until OD<sub>600</sub> reached to 0.4-0.6. The IPTG was added following the optimized concentration. Protein expressions were carried out at 30 °C for 6 hours. Finally, the cell pellets were obtained by centrifugation at 6,000 xg for 10 minutes. The pellets were stored at -80 °C.

### 3.9.3 Purification of bFGF peptide expressed from pET28b-bFGF plasmid

จุฬาลงกรณ์มหาวิทยาลัย

CHULALONGKORN UNIVERSITY

The cell pellet was resuspended in 30 ml in 20 mM Tris, 150 mM NaCl pH 7.5.

Lysozyme (10 mg/ml, 100 µL) was added, and the mixture was incubated at room temperature for 30 minutes, then PMSF (500 µL) was added. Then, the mixture was sonicated using BANDELIN SONOPULS HD 2200 homogenizer, KE76 probe, for 15 seconds, 30% of pulse cycle, and 40% of power and disrupted the mixture until the

mixture became less viscous. The suspension was centrifuged at 40,000 xg, 4 °C for 30 minutes. The supernatant (28.5 ml) mixed with 0.25% of 5% PEI (1.5 ml) and incubated the solution on ice for 5 minutes. The solution was centrifuged at 6,000 xg for 10 minutes and kept the supernatant. After that, the supernatant was dialyzed in 20 mM Tris, pH 7.5. A 2 M of ammonium sulfate ((NH<sub>4</sub>)<sub>2</sub>SO<sub>4</sub>) was added to the solution and kept at room temperature for 5 minutes. After that, the solution was centrifuged at 40,000 xg 4 °C for 15 minutes and kept the supernatant solution. The supernatant was loaded onto Phenyl Hydrophobic column equilibrated in 20 mM Tris, 2 M (NH<sub>4</sub>)<sub>2</sub>SO<sub>4</sub>, pH 7.5. Non-specific binding protein was washed with same buffer. Elution was performed gradient step with 20 mM Tris, changing 2 M to 1 M, 0.5 M, and 0 M (NH<sub>4</sub>)<sub>2</sub>SO<sub>4</sub>. The elution protein fractions were checked by SDS-PAGE and Coomassie Brilliant blue staining. The elution fraction that had target protein were pooled and dialyzed against 20 mM Tris, pH 7.5. Finally, the dialysis solution was purified by fast protein liquid chromatography (FPLC) with SP column that equilibrated in 20 mM Tris, pH 7.5. Elution was performed gradient step with 60% of 20 mM Tris, 1 M NaCl, pH 7.5. The purified protein fractions were checked by SDS-

PAGE and Coomassie Brilliant blue staining. The pure fractions were pooled and dialyzed against 20 mM Tris, pH 7.5. The dialyzed protein was concentrated using centrifugal filter and determined concentration using  $A_{280}$  following by Beer's law

$$A = \epsilon bc$$

Where A is absorbance.

$\epsilon$  is extinction coefficient or molar absorptivity, 15,930  $M^{-1} \text{ cm}^{-1}$  for bFGF as estimated from protein sequence by ExPASy

b is the path length, 1 cm.

c is the concentration of protein in solution.

#### 3.9.4. Purification of bFGF and (GAGAGS)<sub>6</sub>-bFGF expressed from pMALc5x

plasmid

The cell pellet that have bFGF or (GAGAGS)<sub>6</sub>-bFGF was resuspended in 30 ml of buffer A (25 mM HEPES, 150 mM NaCl, and 25 mM Imidazole; pH 7.5). Lysozyme (10 mg/ml, 100  $\mu\text{L}$ ) was added, and the mixture was incubated at room temperature for 30 minutes, then PMSF (500  $\mu\text{L}$ ) was added. Then, the mixture was sonicated

using BANDELIN SONOPULS HD 2200 homogenizer, KE76 probe, for 15 seconds, 30% of pulse cycle, and 40% of power and disrupted the mixture until the mixture became less viscous. The suspension was centrifuged at 40,000  $\times g$ , 4 °C for 30 minutes. The supernatant was loaded onto 3-ml Ni-NTA agarose Beads column equilibrated in buffer A. Non-specific binding protein was washed with buffer A. Elution was performed single step with buffer A changing 25 mM to 250 mM Imidazole. MBP-H<sub>6</sub>-TEV-bFGF or MBP-H<sub>6</sub>-TEV-(GAGAGS)<sub>6</sub>-bFGF was digested with TEV proteinase and 100 mM DTT at 4 °C for 24 hours or until digested completely detected by SDS-gel electrophoresis. After that, the digestive protein was dialyzed in buffer A and purify again in Ni-NTA Agarose Beads column and kept the wash fraction. The purify protein was dialyzed against 20 mM Tris, pH 7.5. The dialysis solution was purified by fast protein liquid chromatography (FPLC) with SP column that equilibrated in 20 mM Tris, pH 7.5. Elution was performed gradient step with 60% of 20 mM Tris, 1 M NaCl, pH 7.5. The purified protein fractions were checked by SDS-PAGE and Coomassie Brilliant blue staining. The pure fractions were pooled and dialyzed against 20 mM Tris, pH 7.5. The dialyzed protein was concentrated using



centrifugal filter and determined concentration using  $A_{280}$  following by Beer's law as described in methodology 3.9.3.

### 3.10 Cell culture

NIH3T3 fibroblast cells were maintained in Dulbecco's modified eagle medium (DMEM) containing 10% fetal bovine serum (FBS) and 1% penicillin/streptomycin. The cells were incubated in a humidified 5%  $CO_2$  atmosphere at 37 °C. The subculture was performed when confluency reached approximately 80-90% using trypsin-EDTA solution to detach the adherent cells.

### 3.11 Optimized concentration of bFGF and (GAGAGS)<sub>6</sub>-bFGF on proliferation of

NIH-3T3

The fibroblast cells were seeded at  $1 \times 10^3$  cells/ml in 96-well plates and incubated in a humidified 5%  $CO_2$  atmosphere at 37 °C overnight for cell attachment.

The DMEM medium was change and treated with various concentration (0, 1, 10, 100 ng/ml) of bFGF and (GAGAGS)<sub>6</sub>-bFGF and incubated for 24 hours. After that, the media was discarded and added the new medium containing MTT solution (10

mg/ml in sterilized water) at the same ratio. The cells were incubated until purple crystal was occurred. Finally, the purple crystals were dissolved by isopropanol and the resulting-colored solution is quantified by measuring of its absorbance at 570 nm light using multi-wells spectrophotometer.

### 3.12. SF hydrogel assembly with optimal concentration of bFGF and (GAGAGS)<sub>6</sub>-

#### bFGF formation

The SF solution was diluted to 4% w/v concentration and sterilized with steam and pressure for 15 minutes and vortexing. After that, the sterilized SF solution (2 ml) mixed with the optimal concentration of bFGF and (GAGAGS)<sub>6</sub>-bFGF in 6 wells plate. The solution was incubated at 37 °C until the hydrogel was occurred.

#### 3.13 *In vitro* bFGF release

The fibroblast cells were seeded at  $1 \times 10^3$  cells/ml in 6-well plates and incubated in DMEM media at 37 °C overnight for cell attachment. The DMEM medium was change and putted four SF containing optimal concentration of growth factor hydrogel cubic (2 mm\*2 mm\*2 mm) and placed at the corner of well and

incubated for 16 days. Medium was changed every day. Every 2 days interval, the

MTT assay was conducted as described in methodology 3.11.



## CHARTER IV

### RESULTS

#### 4.1. Construction of (GAGAGS)<sub>n</sub>-tagged GFP expression plasmids

The DNA sequences coding for the SF repeating unit (GAGAGS) ranging from zero to six repeat unit ((GAGAGS)<sub>n</sub>, n = 0-6) were fused to the DNA sequence of the green fluorescent protein (GFP). TEV-(GAGAGS)<sub>n</sub>-GFP fragments were amplified by polymerase chain reaction (PCR). Detection of the PCR product was analyzed by agarose gel electrophoresis (Fig 5) that TEV-(GAGAGS)<sub>n</sub>-GFP PCR product showed band size between 800 and 900 bps. After purified PCR product, these PCR products and pMALC5x were cut with *NcoI* and *BamHI* restriction enzyme and cloned by ligation process. Then, the ligation reaction was transformed to *E. coli* DH10 $\beta$ . To confirm the cloning result, the transformed *E. coli* DH10 $\beta$  were checked that the TEV-(GAGAGS)<sub>n</sub>-GFP fragments were constructed into the expression plasmid by colony PCR. The positive construction plasmids were extracted and confirmed by nucleic acid sequencing.

The nucleotide sequences analysis showed eight construct plasmid ranging from zero to seven repeat unit (pMALc5x-TEV-(GAGAGS)<sub>n</sub>-GFP, n = 0-7) pMALc5x-TEV-(GAGAGS)<sub>7</sub>-GFP was isolated as a byproduct during the construction of pMALc5x-TEV-(GAGAGS)<sub>6</sub>-GFP, likely by mis-priming during PCR process. The nucleic acid sequence of all gene constructed in pMALc5x plasmid was shown in table 7

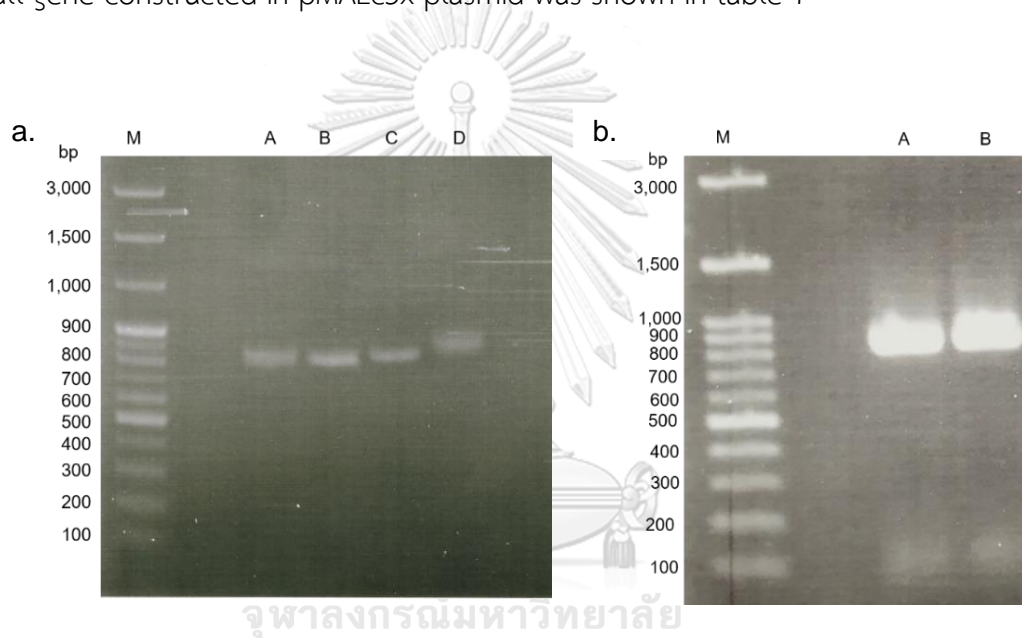


Figure 5: TEV-(GAGAGS)<sub>n</sub>-GFP PCR product in 1% agarose gel. a). M = DNA marker, A = TEV-GFP fragment, B = TEV-GAGAGS-GFP fragment, C = TEV-(GAGAGS)<sub>3</sub>-GFP fragment, D = TEV-(GAGAGS)<sub>6</sub>-GFP fragment. b). M = DNA marker, A = TEV-(GAGAGS)<sub>2</sub>-GFP fragment, B = TEV-(GAGAGS)<sub>5</sub>-GFP fragment.

Table 7: Nucleic acid sequence of TEV-(GAGAGS)<sub>n</sub>-GFP fragment after sequencing analysis

gene	Nucleic acid sequence									
TEV-GFP	catatgtcca	tgggcaaaa	cctgtatttt	cagggttcat	caggtatggt	gagcaaggcc	gaggagctgt	tcaccggggt	ggtgcccatc	
	ctggtcagc	tggacggcga	cgtaaacggc	cacaagtca	gctgtccgg	cgagggcga	ggcgtgcca	cctacggcaa	gctgaccctg	
	aagttcatct	gcaccaccgg	caagctgccc	gtgccctggc	ccaccctcgt	gaccaccctg	acctacggcg	tgcagtgctt	cagccgctac	
	ccgaccaca	tgaagcagca	cgacttcttc	aagtcggcca	tggccgaa	ctacgtccag	gagcgacca	tcttctcaa	ggacgacggc	
	aactacaaga	cccgcggca	ggtgaagttc	gagggcgaca	ccctggtgaa	cgcatcgag	ctgaaaggca	tcgacttcaa	ggaggacggc	
	aacatcctgg	ggcacaagct	ggagtacaac	tacaacagcc	acaagctcta	tatcatggcc	gacaagcaga	agaacggcat	caaggtgaac	
	ttcaagatcc	gccacaacat	cgaagcggc	agcgtcagc	tcggcgacca	ctaccagcag	aacacccca	tcggcgacgg	ccccgtgctg	
	ctgcccgaca	accactacct	gagcaccacg	tcggccctga	gcaaaagacc	caacgagaag	cgcgatcaca	tggctcctgt	ggagttcgtg	
	accgcccgg	ggatcacctt	cggcatggac	gagctgtaca	aggcggcgc	actcgaacac	caccaccacc	accactaata	a	
	catatgtcca	tgggcaaaa	cctgtatttt	caggggtggtg	ctgggtgctgg	ctcaggtgct	ggctctgggt	catcaggtat	ggtgagcaag	
ggcgaaggc	tgttcaccgg	ggtggtgccc	atcctggtcg	agctggacgg	cgacgtagac	ggccacaagt	tcagcgtgtc	cggcgaggggc		
gagggcgatg	ccacctaccg	caagctgacc	ctgaaagtca	tctgcaacc	cggcaagctg	cccgtgacct	ggccccctct	cgtgaccacc		
ctgacctacg	gctgcaagtg	cttcagccgc	taccctgacc	acatgaagca	gcatgacttc	ttcaagtccg	ccatgcccga	aggctacgtc		
cagggcgcca	ccatcttctt	caaggacgac	ggcaactaca	agaccccgcc	cgaagtgaa	ttcgaggggc	acaccctgggt	gaaccgcatc		
gagctgaagg	gcatcgactt	caaggaggac	ggcaacatcc	tggggcaca	gctggagtag	aactacaaca	ggcacaacgt	ctatatcatg		
gcccacaagc	agaagaacgg	catcaagggtg	aacttcaaga	tccggcaca	catcgaaggac	ggcagcgtgc	agctcgccga	ccactaccag		

	<p>cagaacaccc ccatcggcga cgccccgtg ctgtgcccg acaaccacta cctfagcacc caftccgccc ttagcaaga</p> <p>ccccaacgag aagcgcgatic acatggctct gctggafttc gtagaccgcg cggsgatcac tctcggcatg gacgagctgt acaaggcggc</p> <p>cgcactcga g caccaccacc accaccactg ataa</p>
<p>TEV- (GAGAGS)<sub>2</sub>-GFP</p>	<p>catatgtcca tgggcgaaaa cctgtatttt cagsgtggig ctggtgctgg ctcaggtgct caggtgcccgg atctggttca</p> <p>tcaggtatgg tgagcaaggg cgaggagctg ttaccgggg ttgtgcccac cctggtcag ctagaccggc acgtaaacgg ccacaagttc</p> <p>agcgtgtccg gcgaggggca ggcgatgcc acctacggca agctgacct gacttcatc gaafttcatc tgcaccaccg gcaagctgcc cgtgccccfgg</p> <p>cccaccctcg tgaccaccct gactacggc gtgcatgtct tcagccgcta ccccgaccac atggaagcagc acgacttctt caagctccgccc</p> <p>atgccgaa g gctacgtcca gtagcgacc atcttttca agsacgacgg caactacaag acccgcccg aggtgaaagt ctagggcgac</p> <p>accctggtga accgatcga gctgaagggg atcgacttca aggagggacgg caacatcctg ggcacaagc tggagtacaa ctacaacagc</p> <p>cacaacgtct atatcatggc gacaagcag aagaacggca tcaaggatc cttaagatc tcgaggacgg tcgaggacgg cagcgtgca g</p> <p>ctcggcggacc actaccagca gaaccaccac atcggcgacc gcccctgtct gctgtcagc aaccactacc ttagcaccaca gtcccgcccctg</p> <p>agcatagacc ccaacgagaa gcgcatcac atggctctgc tggagttcgt gaccgcccg ggatcactc tcggcatgga ctagctgtac</p> <p>aaggcggccc cactcga gca ccaccaccac caccactgat aa</p>
<p>TEV- (GAGAGS)<sub>3</sub>-GFP</p>	<p>catatgtcca tgggcgaaaa cctgtatttt cagsgtggig ctggtgctgg ctcaggtgct ctggagcagg agcaggaa gt</p> <p>ggtgtggtct ctggttcatc aggtatggig agcaaggcg aggaactgtt caccggggtg gtagccatcc tggctcagct gtagcggcgac</p> <p>gtaacggcc acaagttcag cgtgtcccgc gaggcgagg gcatgcccac ctacggcaag ctgaccctga agttcatctg caccaccggc</p> <p>aa gctgccccg tgcctggccc caccctcgtg accaccctga cctacggcgt gca gctgttc agccgtacc ccgaccacat gaagcagcac</p> <p>gacttttca agtccgccat gcccgaaggc tacgtccagg agcgaccac ctcttcaa g gacgacggca actacaagac ccgcccga g</p> <p>gtgaggttcg agggcgacac cctggtgaac cgtatcagc tgaaggcact gaaaggcga acatctggg gcaacaagtctg gcaacaagtctg</p>

	<p>           gāgtācaact acaaacāgcca caactctat atcatgccc atcatgccc acaagcāgaa gaacggcatc aaggīgaact tcaagatccg            ccacaacatc gaggācggca gctgcaagt cgcgaccac taccāgcaā acaccctcat cggcācggc cccgtgctgc tggcccācaā            ccactacctg āgcaccāgt ccgccctgāg caaagacccc aacgāgāgc gctatcatat ggtccctgctg gāgttcgta cccgccccgg            gatcactctc ggcatggāc āctgtācaā ggccggccgca ctgāgcacc accaccāca ccactgātaā         </p>
<p>           TEV-            (GAGAGS)<sub>4</sub>-GFP         </p>	<p>           catatgtcca tgggcgāaaa cctgtatttt cāgggtggāg cāggāgctgg atcāggāgct gāgctggat cāggāgctgg            āctggāagt ggtgctggg ctggttcāgg tgcāggctcc gāatcatcāg giatgggāg caāgggcgāg gāgctgtca            ccgggtgggt gcccātctg gtcgāgctgg ācggcācgt āaacggccac āggtcācgc tgtccggcga gggcāgaggc            gātgccact ācggcaāgct gāccctgāāg ttcatctgca ccaccggāā gttgcccgtg cctggccca cctctgtagc            caccctgacc tācggctg āgtgcttcāg ccctacccc gāccācatgā āgcāgcācga ctttccaāg tccgccatgc            ccgāaggctā cgtccaaggā cgcaccatct tcttcaaggā cācggcāac tācaāgāccc ggcggāggt gāggtcāg            ggccācāccc tggtaāccg catcāgctg āaggcātgc acttcaāggā gācggāac atcctggggc ācaāgctggā            gtācaactāc ācāgcccāc ācgtctat catggccāc āgcaāgā ggtgāactt āgātccc āgātccc            ācaāctcā gācggcāgc ccgāccāctā cāgācācā accccāctc cāgāgāgc gācācatg cgtgctgctg            cccgācācc āctācctgā cāccāgtcc gccctgācā āgāccāā cāgāgāgc gācācatg tctgctgga            gttctgācc gcccgggā tcaactcgg catggācāg ctgtācāāg cggccgāct cāgācāccā cāccāccāc            actgātaā         </p>
<p>           TEV-            (GAGAGS)<sub>5</sub>-GFP         </p>	<p>           catatgtcca tgggcgāaaa cctgtatttt cāgggtggāg ctggcāgāg ttctggggc ggcctggct            tctggctca ggtgctggg ctggatcgg āgcāggācā gāāgtggg ggtgctg ggtgctg ttcatcāgt atggtgācā            āggcāggā gctgttācc ggggtggtg cctāctggt cācctgāc cāgctggāc ggcgāctāā ācggccāā gttcāgctg         </p>



tccggcggagg	gcgaggggcga	tgccacctac	ggcaagctga	ccctgaagtt	catctgcacc	accggcaagc	tggccgtgccc
ctggcccacc	ctcgtgacca	ccctgacctta	cggcgtgcag	tgtctcagcc	gctaccccga	ccacatgaag	cagcacgact
tcttcaagtc	cggccatgccc	gaaggctacg	tccaggagcg	catcatcttc	ttcaagagcg	acggcaacta	caagaccccgc
gcccgggtga	agttcgaggg	cggacacctg	gtgaaccgca	tcgagctgaa	gggcatcgac	ttcaagggag	acggcaacat
cctggggcac	aagctggagt	acaactacaa	cagccacaac	gtctatatca	tggccgacaa	gagagaagaac	ggcatcaagg
tgaacttcaa	gataccggcac	aacatcgagg	acggcagcgt	gcaactcgcc	gaccactacc	agcagaacac	cccactcggc
gacggccccg	tgtctgtgccc	cgaacaaccac	tacctgagca	cccagtcccgc	cctgagcaaa	gacccccaacg	agaaagcgcga
tcaatgggtc	ctgctggagt	tcgtgaccgc	cggcgggatic	actctcgcca	tggcagagct	gtacaaggcg	ggcgcactcg
agcaccacca	ccaccaccac	tgataa					
catatgtcca	tgggcgaaaa	cctgtatttt	cagggtggtg	ctgggtctgg	ctctggagca	ggagcaggat	ctggggccgg
cgtgggctcg	gggtctgggtg	ctggctcagg	tgtctgtgct	ggatctggag	caggagcagg	aagtgtgct	ggctctggtt
catcagggtat	ggtaggcaag	ggcgaaggagc	tgttcaccgg	ggtagtgccc	atcctggtcg	agctggacgg	cgaagtaaac
ggccacaagt	tcagcgtgtc	cggcgagggc	gagggcgtatg	ccacctacgg	caagctgacc	ctgaaattca	tctgcaccac
cggcaagttg	cccgtgacct	ggcccaccct	cgtgaccacc	ctgacctacg	gctgcaatg	cttcagccgc	taccccgacc
acatgaaaga	gcacgacttc	ttcaagtccg	ccatgcccga	aggctacgtc	caggagcgca	ccatcttctt	caaggacgac
ggcaactaca	agacccgcgc	cgaagtgaag	ttcgaggcg	acacctggt	gaaaccgatic	gagctgaaag	gcatcgactt
caaggaggac	ggcaacatcc	tggggcacaa	gctggagtac	aactacaaca	gccacaacgt	ctatatcatg	ggcgacaagc
agaaagaacgg	catcaagggtg	aacttcaaag	tccgccacaa	catcgaggac	ggcagcgtgc	agctcgccga	ccactaccag
cagaacaccc	ccatcggcga	cggcccctgtg	ctgtgcccg	acaaccacta	cctgagcacc	cagtccgccc	tgagcaaaag

TEV-  
(GAGAGS)<sub>6</sub>-GFP

	ccccaacgag	aagcgcgatc	acatggtcct	gctgggagttc	gtgaccgcgcg	ccgggatcac	tctcggcatg	gacgagctgt
	acaaggcggc	cgcactcgag	caccaccacc	accaccactg	ataa			
	catatgtcca	tggcgaaaa	cctgtatttt	cagggtgag	caaggactgg	atcaggagct	ggagctggat	caggagctgg
	agctggaaat	ggctctggtg	ctggctcagg	tgctgggtct	ggatctggag	caaggagcagg	aagtgggtgca	ggagctggtt
	cagggtctgg	ctctggttca	tcaaggtatgg	tgagcaagg	cgaggagctg	ttcaccgggg	tgggtcccat	cctggctcag
	ctggacggcg	acgtaaacgg	ccacaagttc	agcgtgtccg	gcgagggcga	gggcgatgcc	acctacggca	agctgaccct
	gaagttcatc	tgcaccaccg	gcaagttgcc	cggtccctgg	cccaccctcg	tgaccaccct	gacctacggc	gtgcagtgct
	tcagccgcta	ccccgaccac	atgaaagcagc	acgacttctt	caagtccgcc	atgcccgaag	gctacgtcca	ggagcgcacc
	atcttcttca	aggacgacgg	caactacaag	accgcgcgcg	aggtgaagtt	cgagggcgac	accctgggtga	accgcatcga
	gctgaaaggc	atcgacttca	aggagggcgg	caacatcctg	gggcacaagc	tggagtacaa	ctacaacagc	cacaacgtct
	atatcatggc	cgacaagcag	aaggaaaggca	tcaagggtgaa	cttcaagatc	cgccacaaca	tcgaggagcgg	cagcgtgcag
	ctcggcgacc	actaccagca	gaacaccccc	atcggcgagc	gccccgtgct	gctgcccgac	aaccactacc	tgagcaccca
	gtccgcccctg	agcaaaagacc	ccaacgagaa	gcgcgatcac	atggtctctgc	tggagttcgt	gaccgcccgc	gggatcactc
	tcggcatgga	cgagctgtac	aaggcggccg	cactcggca	ccaccaccac	caccactgat	aa	

TEV-  
(GAGAGS)<sub>7</sub>-GFP

Table 8: Amino acid sequence of recombinant peptides

Recombinant peptides	Amino acid sequence										
TEV-GFP-H <sub>6</sub>	MSMGENLYFQ	GSSGMVSKGE	ELFTGVVPII	VELDGDVNGH	KFSVSGEGEG	DATYGKLTlk	FICTTGKLPVP				
	WPTLVTTlTY	GVQCFSRYPD	HKQHdFFKSA	MPEGYVQERT	IFFKDDGNyK	TRAEVkfEGD	TLVnRIELKq				
	IDFKEDGNIL	GhKLEyNYNS	HNvYIMADKQ	KNGIKvNFkI	RHNIEDGSVQ	LADHYQqNTP	IGDGPVLLPD				
	NHYLSTQsAL	SKDPNEKRdH	MVLLFTAAg	ITLGMDELyK	AAALEHhHHHh	H					
TEV-GAGAGS-GFP-H <sub>6</sub>	MSMGENLYFQ	GAGAGSGAG	SGSSGMVSKG	EELFTGVVPI	LVELDGDVDG	HKFSVSGEGE	GDATYGKLTl				
	KFICTTGKLP	VPWPTLVTTl	TYGVQCFSRY	PDHMKQHdFF	KSAMPEGYVQ	ERTIFFKDDG	NYKTRAEVkf				
	EGDTLVNRIE	LKGIDFKEDG	NILGHKLEyN	YNSHNvYIMa	DKQKNGIKvN	FKIRHNIEDG	SVQLADHYQq				
	NTPIGDGPVL	LPDNHylSTQ	SALSKDPNEK	RDHMVLLFEV	TAAPGITLGM	DELYKAAALE	HHHHHHh				
TEV-(GAGAGS) <sub>2</sub> -GFP-H <sub>6</sub>	MSMGENLYFQ	GAGAGSGAG	AGSGAGSGSS	GMVSKGEELF	TGVVPIlVEL	DGDVNGHKFS	VSGEGEGDAT				
	YgKLTlKfIC	TtGKLpVpWP	TLVTTlTYGV	QCFSRYPDHM	KQHdFFKSAM	PEGYVQERTI	FFKDDGNyKT				
	RAEVkfEGDT	LVNRIELKGI	DFKEDGNILG	HKLEyNYNSH	NVYIMADKQK	NGIKvNFkIR	HNIEDGSVQL				
	ADHYQqNTTI	GdGPVLLLDN	HYLSTQsALS	IDPNEKRdHM	VLLFEVTAAG	ITLGMDELyK	AAALEHhHHHh				
TEV-(GAGAGS) <sub>3</sub> -GFP-H <sub>6</sub>	MSMGENLYFQ	GAGAGSGAG	AGSGAGSGG	AGSSSGMVS	KGEELFTGVV	PILVELDGDV	NGHKFSVSGE				
	GEGDATYgKL	TlKfICTTGK	LpVpWPTLVt	TLTYGVQCFS	RYPdHMKQHd	FFKSAMPEGY	VQERTIFFKd				

	DGNYKTRAEV KFEQDGLVNR IELKIDFKE DGNILGHKLE YNNSHNYVI MADKQKNGIK VNFKIRHNIE DGSVQLADHY QONTTIGDGP VLLLDNHYS TQSALSIDPN EKRDMVLE EFTAAAGITLG MDELYKAAAL EHHHHHHH
TEV-(GAGAGS) <sub>4</sub> - GFP-H <sub>6</sub>	MSMGENLYFQ GGAGAGSGAG AGSGAGSGG AGAGSGAGSG SSGMVSKEE LFTGVVPIV ELDDGVNGHK FSVSGEGED ATYGKLTLEF ICTTGKLPVP WPTLVTTLY GVQCFSRYPD HMKQHDFFKS AMPEGYVQER TIFFKDDGNY KTRAEVKFEG DTLVNRIELK GIDFKEDGNI LGHKLEYNYN SHNVYIMADK QKNGIKVNFK IRHNIEDGSV QLADHYQQNT TIGDGPVLLL DNHYLSTQSA LSIDPNEKRD HMLLEFVTA AGITLGMDEL YKAAALEHHH HHH
TEV-(GAGAGS) <sub>5</sub> - GFP-H <sub>6</sub>	MSMGENLYFQ GGAGAGSGAG AGSGAGSGG AGAGSGAGAG SGAGSGSGM VSKGEELFTG VVPIVELDG DVNGHKFSVS GEGEGDATYG KLTLEKICTT GKLVPWPPTL VTTLTYGVQC FSRYPDHMKQ HIDFFKSAMPE GYQERTIFF KDDGNYKTRA EVKFEQDGLV NRIELKIDF KEDGNILGHK LEYNYNSHNV YIMADKQKNG IKVNFKIRHN IEDGSVQLAD HYQQNTTIGD GPVLLLDNHY LSTQSALSID PNEKRDHMLV LEFVTAAGIT LGMDELYKAA ALEHHHHHHH
TEV-(GAGAGS) <sub>6</sub> - GFP-H <sub>6</sub>	MSMGENLYFQ GGAGAGSGAG AGSGAGSGG AGAGSGAGAG SGAGAGSGAG SGSSGMVSKG EELFTGWPI LVELDGDVNG HKFSVSGEGE GDATYKGLTL KFICITGKLP VPWPTLVTTL TYGVQCFSRY PDHMKQHDFD KSAMPEGYVQ ERTIFFKDDG NYKTRAEVKF EGDTLVNRIE LKIDFKEDG NILGHKLEYN YNSHNVYIMA DKQKNGIKVN FKIRHNIEDG SVQLADHYQQ NTTIGDGPVL LLDNHYSTQ SALSIDPNEK RDHMLLEFV TAAGITLGM D ELYKAAALEH HHHHH
TEV-(GAGAGS) <sub>7</sub> -	MSMGENLYFQ GGAGAGSGAG AGSGAGSGG AGAGSGAGAG SGAGAGSGAG AGSGAGSGSS GMVSKGEELF

GFP-H <sub>6</sub>	TGWPILEVEL	DGDVNGHKFS	VSGEGEGDAT	YGKLTCLKFIC	TTGKLPVPWP	TLVTTLTYGV	QCFSRYPDHIM
	KQHDFFKSAM	PEGYVQERTI	FFKDDGNYKT	RAEVKFEEDT	LVNRIELKGI	DFKEDGNILG	HKLEYNYNSH
	NVYIMADKQK	NGIKVNFKIR	HNIEDGSVQL	ADHYQQNTTI	GDGPVLLLDN	HYLSTQSALS	IDPNEKRDHIM
	VLLEFVTAAG	ITLGMDELYK	AAALEHHHHH	H			



## 4.2 (GAGAGS)<sub>n</sub> tagged GFP protein expression and purification

After plasmid construction and DNA sequence verification, the (GAGAGS)<sub>n</sub>-GFP peptide expressed using the *E. coli* host for large scale production. After (GAGAGS)<sub>n</sub>-GFP peptide large scale production, the peptide needed to be purified and concentrated. First, the peptide supernatant from sonication was purified using Ni-NTA agarose column. Then, TEV protease was added to MBP-TEV-(GAGAGS)<sub>n</sub>-GFP fraction for digested at TEV site. After that, the digestive peptide was purified again with Ni-NTA agarose column. The (GAGAGS)<sub>n</sub>-GFP peptide was purified with Q-Sepharose column because these peptides had negative charge. After concentration using centrifugal filter, the peptide purity was checked by the SDS-PAGE and showed the (GAGAGS)<sub>n</sub>-GFP band around 25-28 kDa (Fig 6) and concentration was determined by Bradford assay. The (GAGAGS)<sub>n</sub>-GFP peptide concentration was calculated using linear regression formula of standard curve (shown in appendix) and concentration of this peptide was shown in table 9.

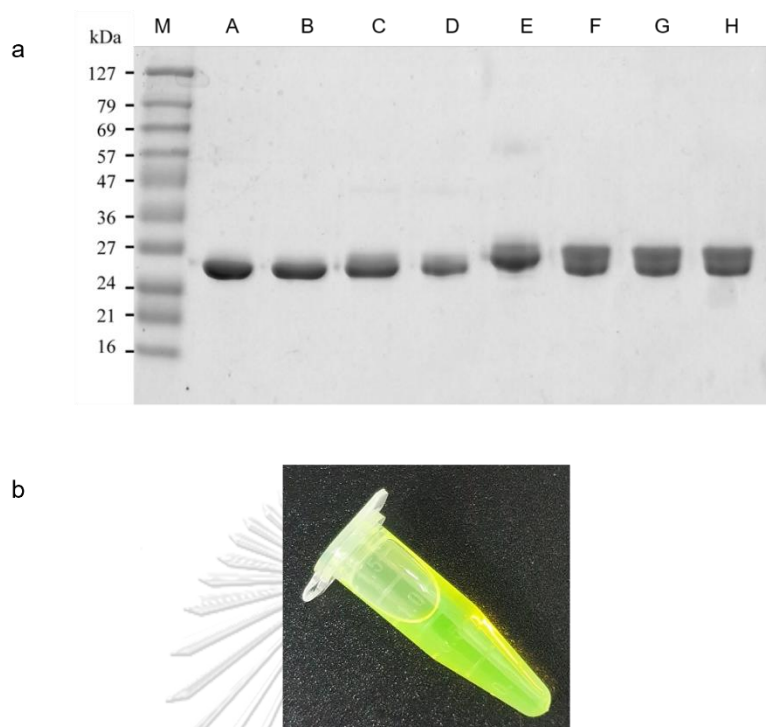


Figure 6: SDS-PAGE of purified recombinant  $(GAGAGS)_n$ -GFP peptide (a) and purified recombinant  $(GAGAGS)_n$ -GFP peptide (b). M = protein marker; A = GFP; B = GAGAGS-GFP; C =  $(GAGAGS)_2$ -GFP; D =  $(GAGAGS)_3$ -GFP; E =  $(GAGAGS)_4$ -GFP; F =  $(GAGAGS)_5$ -GFP; G =  $(GAGAGS)_6$ -GFP; and H =  $(GAGAGS)_7$ -GFP respectively

Table 9: Concentration of  $(GAGAGS)_n$ -GFP peptide by Bradford assay

Peptides	Concentration (mg/ml)
GFP	8.28
GAGAGS-GFP	7.05
$(GAGAGS)_2$ -GFP	7.89
$(GAGAGS)_3$ -GFP	8.04
$(GAGAGS)_4$ -GFP	5.56
$(GAGAGS)_5$ -GFP	6.69
$(GAGAGS)_6$ -GFP	6.83
$(GAGAGS)_7$ -GFP	9.32

### 4.3 Formation of SF/(GAGAGS)<sub>n</sub>-GFP hydrogel

Determination time of SF hydrogel was performed in 96-well microplate that each well composed of vortexed SF solution and (GAGAGS)<sub>n</sub>-GFP at the same volume and final concentration adjusted to 4% w/v of SF solution and 100  $\mu\text{g/ml}$  of (GAGAGS)<sub>n</sub>-GFP peptides. The solution was incubated at 37 °C and measured absorbance at 550 nm wavelength every 2 hours. The gelation time results were showed in fig 7 and table 10. The SF solution with (GAGAGS)<sub>5</sub>-GFP, (GAGAGS)<sub>6</sub>-GFP, and (GAGAGS)<sub>7</sub>-GFP formed hydrogels within 55 hours. After 58 hours of experiment time, the SF solution with (GAGAGS)<sub>2</sub>-GFP, (GAGAGS)<sub>3</sub>-GFP and (GAGAGS)<sub>4</sub>-GFP formed hydrogel. In addition, the condition of SF with GAGAGS-GFP and untagged GFP formed hydrogel within 72 hours. Finally, the SF solution alone showed the latest of forming hydrogel. The results in this experiment concluded that increasing the repeat unit of SF (GAGAGS) could reduce the gelation time of SF hydrogel.



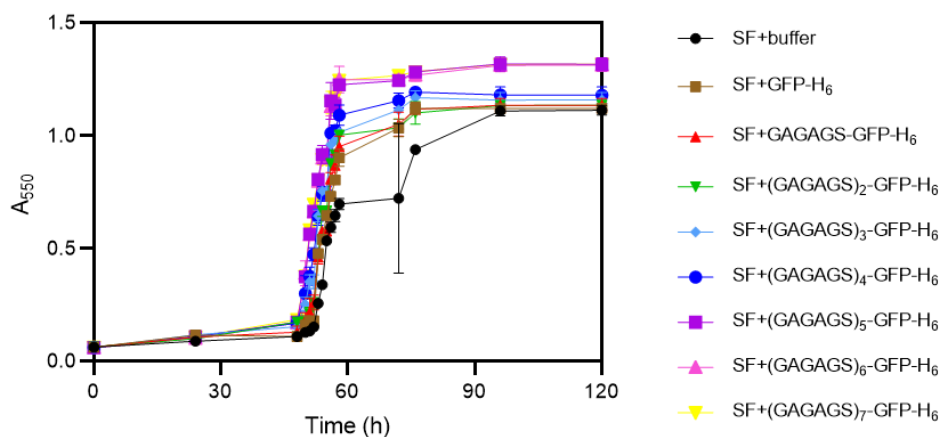


Figure 7: The gelation time of SF hydrogel in different of  $(GAGAGS)_n$ -GFP peptides.

Table 10: The gelation time point of SF solution with  $(GAGAGS)_n$ -GFP peptides formed hydrogel.

Conditions	Gelation time point of SF hydrogel
SF+buffer	96 hours
SF+GFP	72 hours
SF+GAGAGS	72 hours
SF+(GAGAGS) <sub>2</sub> -GFP	58 hours
SF+(GAGAGS) <sub>3</sub> -GFP	58 hours
SF+(GAGAGS) <sub>4</sub> -GFP	56 hours
SF+(GAGAGS) <sub>5</sub> -GFP	55 hours
SF+(GAGAGS) <sub>6</sub> -GFP	55 hours
SF+(GAGAGS) <sub>7</sub> -GFP	55 hours

Decreasing of  
gelation time

#### 4.4. *In vitro* release of GFP from SF hydrogel

To explore the release profile of GFP from SF hydrogel, the GFP release was determined by its absorbance at 395 nm light. Interestingly, , the absorbance of GFP that release from SF hydrogel assembly with GFP, GAGAGS-GFP, and (GAAGS)<sub>2</sub>-GFP occurred the fastest equilibrium value with 10 minutes and this value stable until the end of experiment (Fig 8a). While the GFP that release from SF/(GAGAGS)<sub>3</sub>-GFP and SF/(GAGAGS)<sub>4</sub>-GFP hydrogel showed the highest of absorbance value and reached the equilibrium within 80 minutes still equilibrated until the end of testing (Fig 8a). Interestingly, the SF hydrogel with (GAGAGS)<sub>5</sub>-GFP, (GAGAGS)<sub>6</sub>-GFP, and (GAGAGS)<sub>7</sub>-GFP showed gradually increase of GFP absorbance and occurred the highest value and reached the equilibrium within at 48 hours (2,880 minutes), 72 hours (4,320 minutes), and 96 hours (5,760 minutes) respectively (Fig 8b).

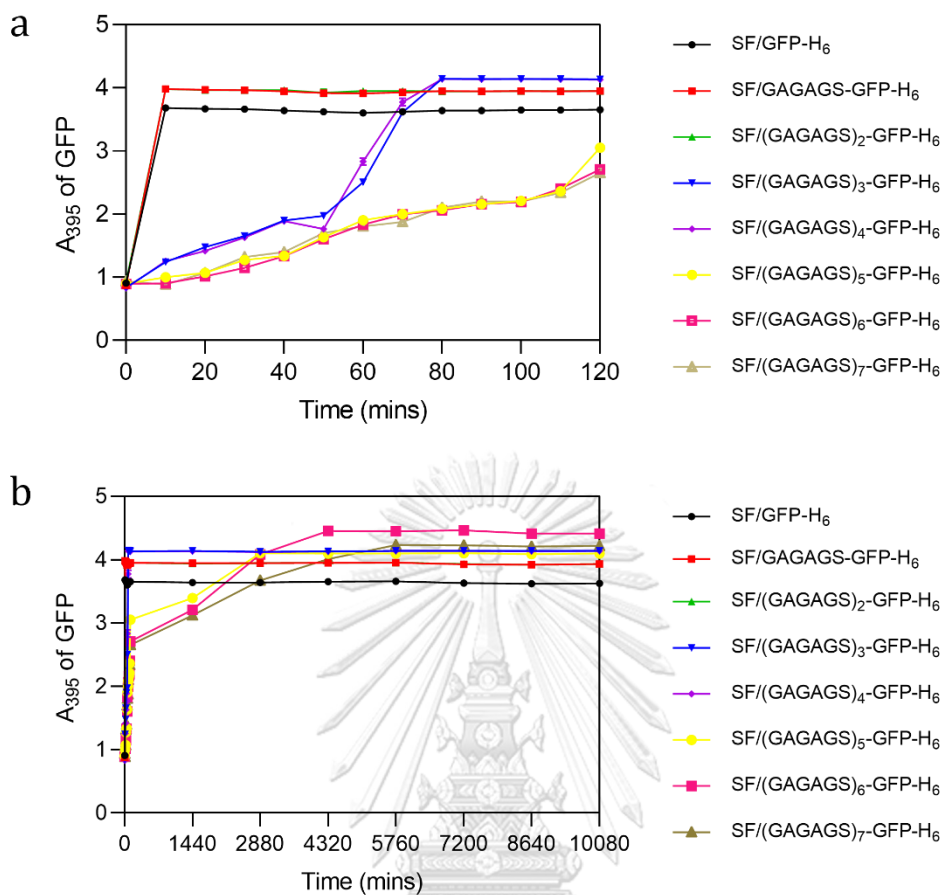


Figure 8: In vitro release profiles of the recombinant GFP from the SF hydrogels

#### 4.5 In vitro enzymatic degradation of SF/(GAGAGS) $_n$ -GFP hydrogel

To explore the effect of repeating unit on degradation of SF hydrogel, the hydrogels were submerged in PBS buffer that containing 1 U/ml protease XIV. Generally, the SF hydrogel was not easily degraded in normal environment without specific enzyme because it had high beta-sheet content. After 30 days, the SF hydrogel containing (GAGAGS) $_5$ -GFP, (GAGAGS) $_6$ -GFP, and (GAGAGS) $_7$ -GFP remained the

weight of hydrogel cube upper 50% of gel weight compare in first day (Fig 9). In contrast, the condition had GFP, GAGAGS-GFP, (GAGAGS)<sub>2</sub>-GFP showed the lowest of weight SF hydrogel (Fig 9). And the sample of (GAGAGS)<sub>3</sub>-GFP, and (GAGAGS)<sub>4</sub>-GFP hydrogel remained weight of SF hydrogel around 20-30% that showed in Fig 9. These results indicated that the degradation rate of SF hydrogels contained varying of repeat unit depended on the number of silk fibroin repeat unit(s).

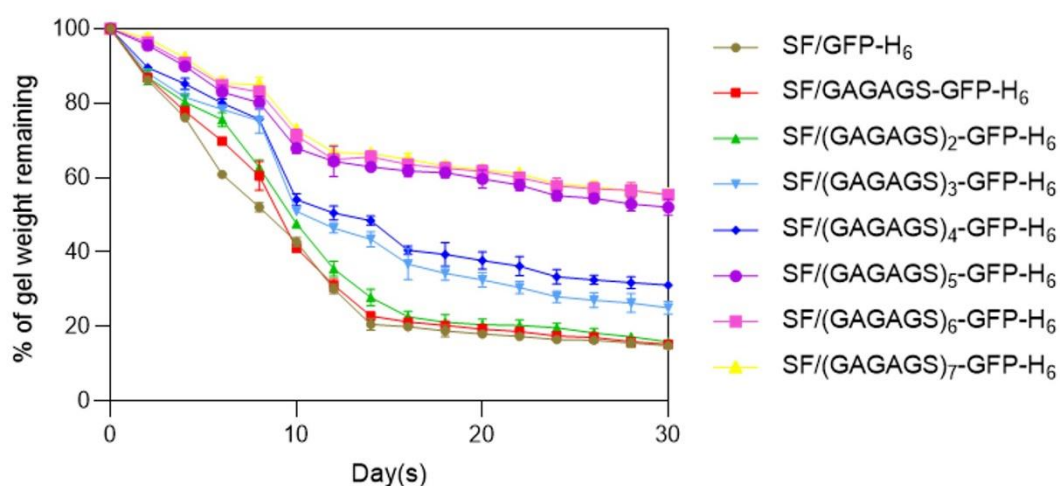


Figure 9: SF hydrogel degradation profile was showed the percentage of SF/(GAGAGS)<sub>n</sub>-GFP hydrogels weight remaining that incubated in protease XIV (1 U/ml) solution at 37 °C around 30 days.

#### 4.6 Characterization of SF/(GAGAGS)<sub>n</sub>-GFP lyophilized hydrogel

SF protein secondary structure was analyzed by Fourier Transform Infrared spectroscopy (FTIR) and X-ray diffraction (XRD). FTIR was a common tool for analysis the molecular structure conformation. Normally, SF secondary structure had four main structures; random coil, alpha-helix, beta-sheet, and beta turn especially beta-sheet and random coil structure were a major structure in SF protein. The spectrum wavenumber of SF hydrogel mixed GFP, GAGAGS-GFP, (GAGAGS)<sub>3</sub>-GFP, and (GAGAGS)<sub>6</sub>-GFP demonstrated peak slightly shifted the amide I absorption peaks from 1650 cm<sup>-1</sup> (random coils) toward 1630 cm<sup>-1</sup> ( $\beta$ -sheet). However, the shift in the amide II absorption was unclear (Fig 10). This result suggested that longer repeating unit (GAGAGS) induced more crystalline  $\beta$ -sheet formation.

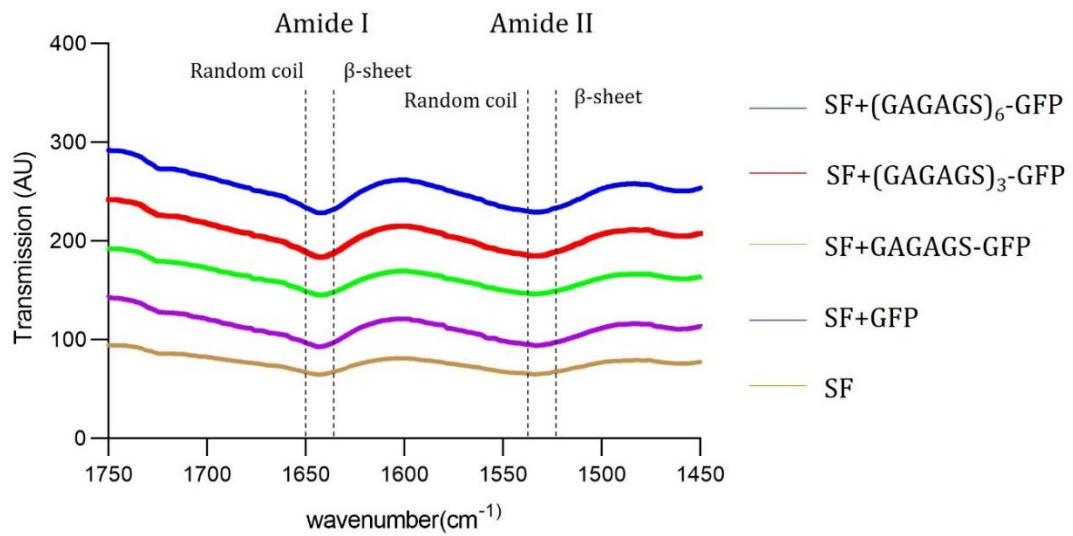


Figure 10: Fourier-transform infrared spectroscopy (FTIR) spectra of SF hydrogel around the absorption bands of amide I and amide II

Another tool for analysis SF protein structure was X-ray diffraction (XRD). The crystalline of SF protein mainly occurred peak around  $19.5 - 22.5^\circ$ . The spectrum XRD results showed peak at  $22.36^\circ$  for SF,  $19.62^\circ$  for SF+GFP,  $21.19^\circ$  for SF+GAGAGS-GFP,  $20.76^\circ$  for SF+(GAGAGS)<sub>3</sub>-GFP and  $21.07^\circ$  for SF+(GAGAGS)<sub>6</sub> (Fig 11). These results showed that the peak in XRD spectra represented crystalline region or beta-sheet

structure were increased with increasing number of repeat units

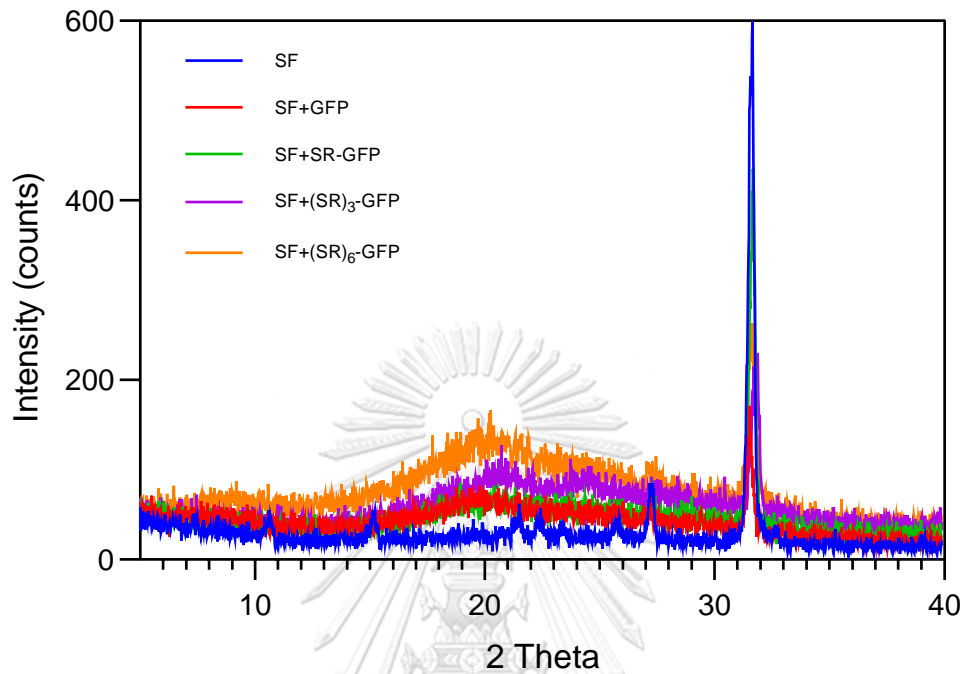


Figure 11: X-ray diffraction (XRD) pattern from  $5^{\circ}$  –  $40^{\circ}$  of SF hydrogel

#### 4.7 Construction of (GAGAGS)<sub>n</sub>-tagged bFGF expression plasmids

The DNA sequences coding for the SF repeating unit (GAGAGS) of zero and six repeat unit were fused to the DNA sequence of basic fibroblast growth factor (bFGF). TEV-(GAGAGS)<sub>n</sub>-bFGF fragments was amplify by polymerase chain reaction (PCR). Detection of the PCR product was analyzed by agarose gel electrophoresis (Fig 12) that bFGF and TEV-bFGF PCR product showed size band between 400 to 600 bp.

After PCR product purification, pET28b and pMALC5x were cut with *NcoI* and *HindIII* restriction enzyme and the PCR product cloned into by ligation. Then, the ligation reaction was transformed to *E. coli* DH10 $\beta$ . To confirm the cloning result, the transformed *E. coli* DH10 $\beta$  were checked that the TEV-(GAGAGS)<sub>n</sub>-GFP fragments were constructed into the expression plasmid by colony PCR. The positive construction plasmids were extracted and confirmed by nucleic acid sequencing. The nucleic acid sequencing of bFGF fragment in pET28b plasmid and TEV-bFGF fragment in pMALc5x were shown in table 11 and the amino acid sequences that translated from the nucleic acid sequencing was shown in table 12.

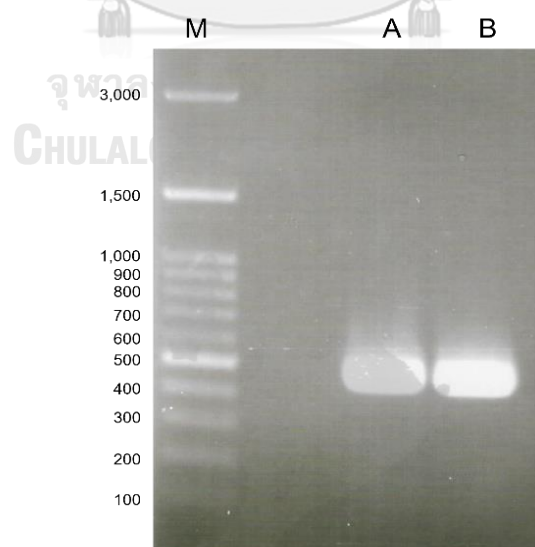


Figure 12: TEV-bFGF in lane A and bfgf in lane B PCR product in 1% agarose gel.



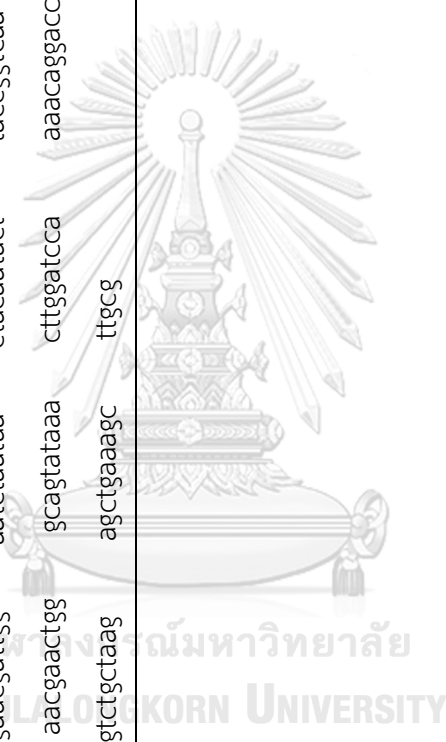
pMALc5x-TEV-(GAGAGS)<sub>6</sub>-bFGF plasmid was synthesized and purchased from Biomatik company. The DNA sequences of bFGF-(GAGAGS)<sub>6</sub>-bFGF fragment was showed in table 11 and the amino acid sequences that was translated from the nucleic acid sequencing was shown in table 12.



Table 11: DNA sequence of bFGF, TEV-bFGF, and TEV-(GAGAGS)<sub>6</sub>-bFGF fragment

Fragment	DNA sequence													
bFGF	ataccatggc	agccgggagc	atcaccacgc	tgccgcctt	gcccggaggat	ggggcagcg	ggccttccc	gcccggccac	tcaaggacc	ccaagcggct	gtactgcaaa	aacggggct	tcttctgcg	catccacccc
	gacggccgag	ttgacgggt	ccgggagaag	agcaccctc	acatcaagct	acaactcaa	gcagaagaga	gaggattgt	gtctataaa	ggagtgtg	ctaaccgta	cctggctatg	aaggaagatg	gaagattact
	ggcttctaaa	tggttacgg	atgagtgtt	ctttttgaa	cgattggaat	ctaataacta	caatacttac	cggtcaagga	aatacaccag	ttgatatgtg	gactgaaac	gaactgggca	gtataaactt	ggatccaana
	caggacctgg	gcagaagct	atacttttc	ttccaatgct	tgctaagagc	tgaaaactt	cg							
TEV-bFGF	ataccatggg	acaccaccac	caccaccacg	gttccgaaaa	cctgtatttt	caagggggtg	ctggctctgg	ttcatcaggt	atggcagccg	ggagcatcac	cacgctgcc	gccttgcccg	aggatggcg	cagcggcggc
	ttcccggccc	gcccactcaa	ggaccccaag	cggctgtact	gcaaaaaacgg	ggcttcttc	ctgscgatcc	accccgacgg	ccgagttgac	gggtccggg	agaagagcga	ccctcacatc	aagctacaac	ttcaagcaga
	agagagagga	gttgtgtcta	tcaaaggagt	gtgtgctaac	cgttaccctgg	ctatgaaaga	agatggaaga	ttactggctt	ctaaatgtgt	tacggatgag	tgtttctttt	ttgaaagatt	ggaattaat	aactacaata
	cttaccggtc	aaggaatac	accagtgtgt	atgtggcact	gaaacgaact	ggcagata	aacttggatc	caaaacaagga	cctggcaga	aagctatact	ttttctcca	atgtctgcta	agagctgaaa	gcttgcg
TEV- (GAGAGS) <sub>6</sub> -bFGF	ataccatggg	acaccaccac	caccaccacg	gttccgaaaa	cctgtatttt	caagggcggg	ctggagcggg	ctctggggcc	ggcgtggct	cgggtgtgag	agccgctct	gggcccggcg	ctggctcggg	ggcaggaagcc

gggtctggag	caggagcagg	aagtgggtct	ggctctggtt	catcaggtat	ggcagccggg	agcatcacca
cgtgcccgc	cttgcccgag	gatggcgga	gcgggcctt	cccggccggc	cactcaagg	acccaagcg
gctgtactgc	aaaaacgggg	gcttctct	gcgatccac	cccgacggc	gagttgacgg	ggtcgggag
aagagcacc	ctcacatcaa	gctacaactt	caagcagaag	agagggagt	tgtgtctatc	aaaggagtgt
gtgctaaccg	ttacctggt	atgaaggaa	atggaagatt	actggcttct	aaatgtgta	cgsatgagtg
ttctttttt	gaacgattgg	aatctaataa	ctacaatact	taccggtcaa	ggaatacac	cagttggtat
gtggcactga	aacgaaactgg	gcagataaaa	cttggatcca	aaacaggacc	tggcagaaa	gctatacttt
ttctccaat	gtctgctaag	agctgaaagc	ttgcg			



จุฬาลงกรณ์มหาวิทยาลัย  
CHULALONGKORN UNIVERSITY

Table 12: Amino acid sequence of bFGF, TEV-bFGF and TEV-(GAGAGS)<sub>6</sub>-bFGF peptides.

Peptide	Amino acid sequence					
bFGF	MAAGSITLTP	ALPEDGGSGA	FPPGHFKDPK	RLYCKNGGFF	LRIHPDGRVD	GVREKSDPHI
	KLQLQAEERG	WSIKGVCAN	RYLAMKEDGR	LLASKCVTDE	CFFFERLESN	NYNTYRSRKY
	TSWYVALKRT	GQYKLGSKTG	PGQKAILFLP	MSAKS		
H <sub>6</sub> -TEV-bFGF	MGHHHHHHGS	ENLYFQGGAG	SGSSGMAAGS	ITTLPALPED	GGSGAFPPGH	FKDPKRLYCK
	NGGFFLRIHP	DGRVDGVREK	SDPHIKLQLO	AEERGWSIK	GVCANRYLAM	KEDGRLLASK
	CVTDECEFFE	RLESNNYNTY	RSRKYTSWYV	ALKRTGQYKL	GSKTGPQOKA	ILFLPMSAKS
H <sub>6</sub> -TEV-(GAGAGS) <sub>6</sub> -bFGF	MGHHHHHHGS	ENLYFQGGAG	AGSGAGAGSG	AGAGSGAGAG	SGAGAGSGAG	AGSGAGSGSS
	GMAAGSITTL	PALPEDGGSG	AFPPGHFKDP	KRLYCKNGGF	FLRIHPDGRV	DGVREKSDPH
	IKLQLQAEER	GWSIKGVCA	NRYLAMKEDG	RLLASKCVTD	ECFFFERLES	NNNTYRSRK
	YTSWYVALKR	TGQYKLGSKT	GPGQKAILFL	PMSAKS		

## 4.8 bFGF, H<sub>6</sub>-TEV-bFGF and H<sub>6</sub>-TEV-(GAGAGS)<sub>6</sub>-bFGF expression and purification

### 4.8.1 bFGF expression and purification

bFGF expression using *E. coli* was optimized for an appropriate IPTG concentration. The result, shown in Fig 13, indicated that bFGF expressed as high amount of soluble protein. Even though the bFGF expression can be detected without inducing by IPTG, IPTG (0.1  $\mu$ M) was used in large scale production.

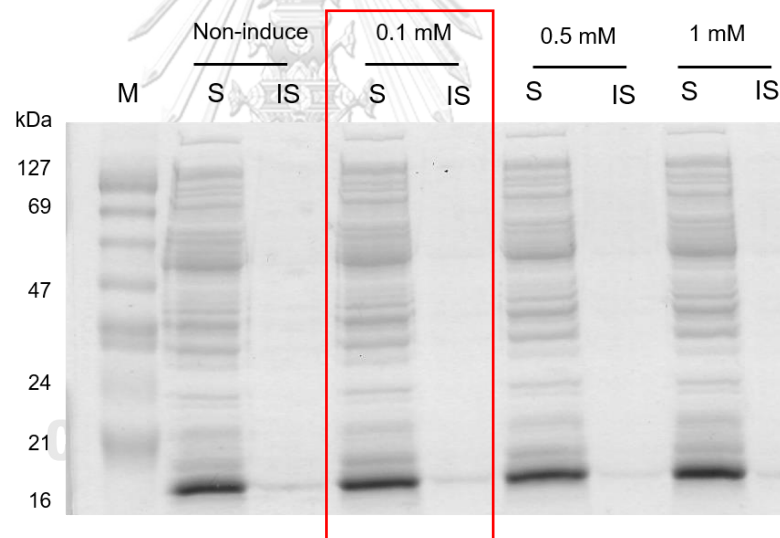


Figure 13: The optimization of IPTG varying on IPTG concentration. M = protein marker, S = soluble protein (from supernatant sample), IS = insoluble protein (from cell debris sample)

After bFGF large scale production, soluble protein was extracted and kept the supernatant for purify step. The 0.25% of PEI solution was added into supernatant for precipitated contaminant protein Fig 14.

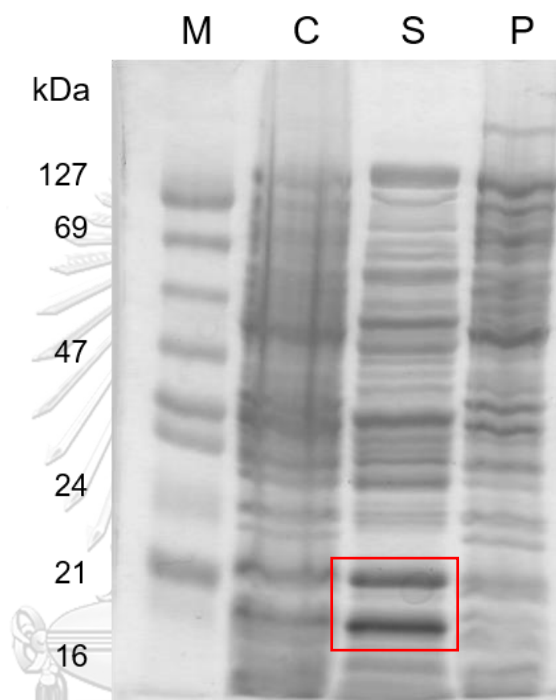


Figure 14: The PEI precipitate purification in 0.25% v/v concentration. M = protein marker, C = crude protein, S = soluble protein, P = precipitated protein; The SDS-PAGE result shows the bFGF band around 16-21 kDa in soluble fraction that show the higher intensity band.

After precipitation, the supernatant was collected and precipitated again with 2 M of ammonium sulfate ((NH<sub>4</sub>)<sub>2</sub>SO<sub>4</sub>) to precipitate impurity component. Then

supernatant was purified by hydrophobic interaction chromatography. The bFGF peptide can bind to hydrophobic column and eluted with gradient step of  $(\text{NH}_4)_2\text{SO}_4$  from 2 M concentration to 0 M concentration of  $(\text{NH}_4)_2\text{SO}_4$ . The hydrophobic result is shown in Fig 15. In this case, the  $E_1$ - $E_3$  of eluted bFGF were selected.

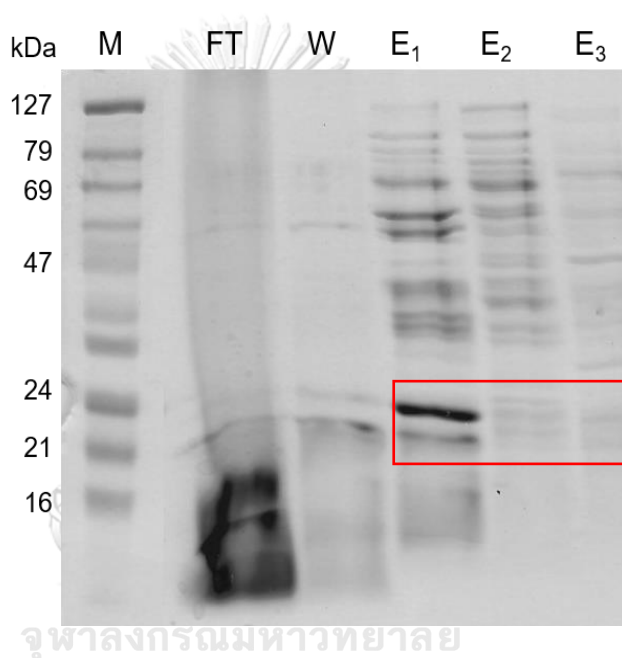


Figure 15: The purification of bFGF peptide by hydrophobic column. M = protein marker, FT = protein in 2 M  $(\text{NH}_4)_2\text{SO}_4$ , W = wash fraction with 2 M  $(\text{NH}_4)_2\text{SO}_4$ ,  $E_1$  = wash fraction with 1 M  $(\text{NH}_4)_2\text{SO}_4$ ,  $E_2$  = wash fraction with 0.5 M  $(\text{NH}_4)_2\text{SO}_4$ ,  $E_3$  = wash fraction with 0 M  $(\text{NH}_4)_2\text{SO}_4$

After gradient elution, the bFGF was purified with ion-exchange chromatography. Before purified this peptide, the peptide was dialyzed in 20 mM

Tris, pH 7.5 for remove  $(\text{NH}_4)_2\text{SO}_4$ ). Then, the peptide purified with SP column and the peptide purity was shown in Fig 16. In this case, the  $F_{29}$ - $E_1$  fractions of eluted bFGF were selected. After concentration using centrifugal filter, the peptide concentration was determined using  $A_{280}$  following by Beer's law and shown the concentration in table 16

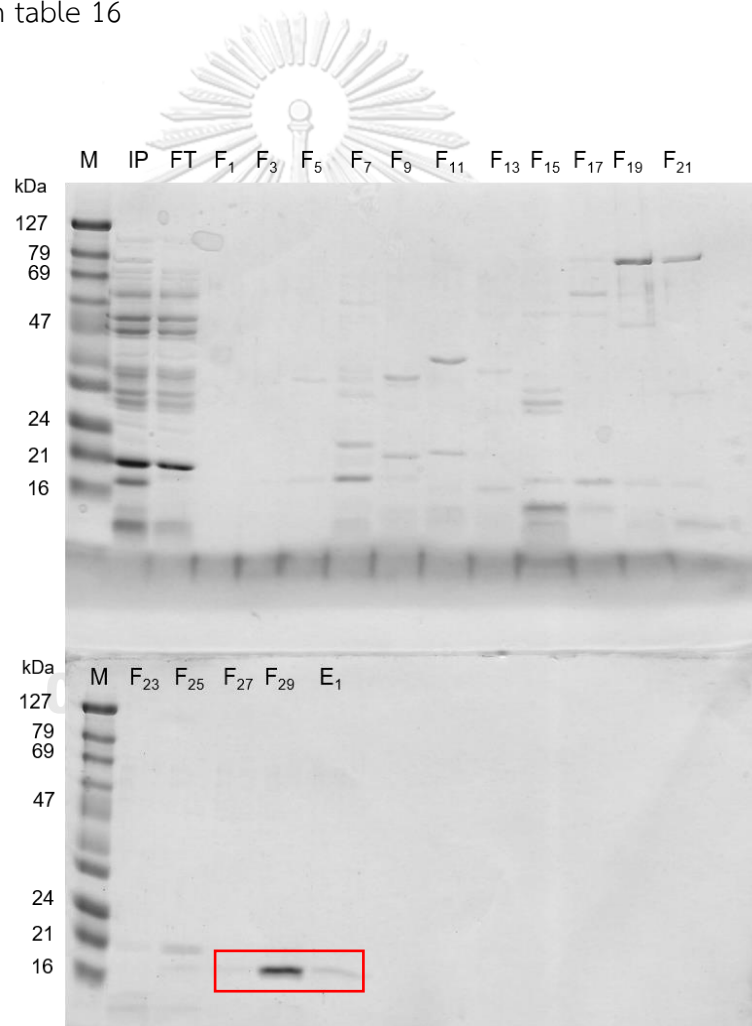


Figure 16: The bFGF purification by ion-exchange chromatography. M = protein marker, IP = protein input solution, FT = protein unbonded solution,  $F_1$ - $F_{29}$  = bFGF eluted fraction of 0 mM – 1 M NaCl concentration,  $E_1$  = eluted fraction in 1 M NaCl



#### 4.8.2 H<sub>6</sub>-TEV-bFGF and H<sub>6</sub>-TEV-(GAGAGS)<sub>6</sub>-bFGF expression

H<sub>6</sub>-TEV-bFGF and H<sub>6</sub>-TEV-(GAGAGS)<sub>6</sub>-bFGF expression using *E. coli* were optimized the IPTG concentration. The results, shown in Fig 17, indicated that H<sub>6</sub>-TEV-bFGF (Fig 17a) and H<sub>6</sub>-TEV-(GAGAGS)<sub>6</sub>-bFGF (Fig 17b) expressed as high amount of soluble protein. Even though the (His)<sub>6</sub>-TEV-bFGF and H<sub>6</sub>-TEV-(GAGAGS)<sub>6</sub>-bFGF expression can be detected without inducing by IPTG, IPTG (0.1 μM) was used in large scale production.

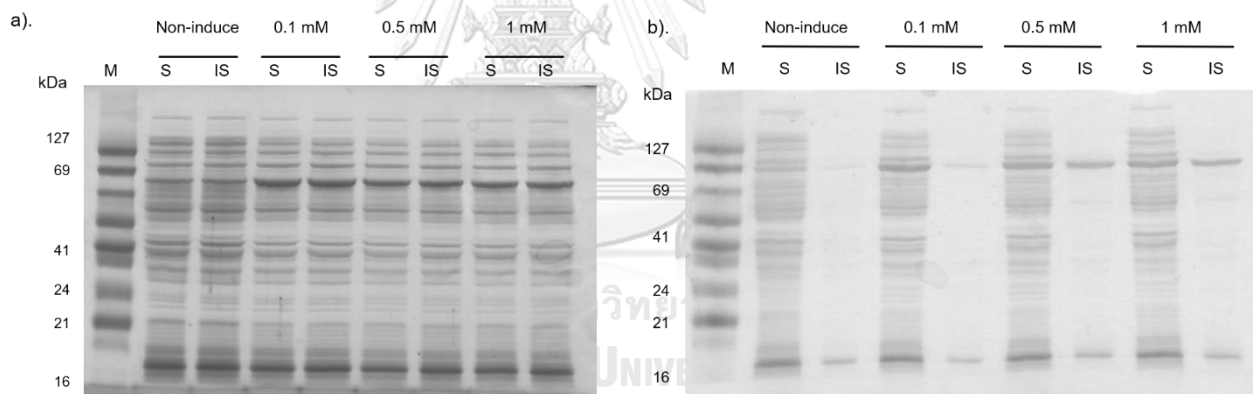


Figure 17: The optimization of IPTG varying on IPTG concentration. M = protein marker, S = soluble protein (from supernatant sample), IS = insoluble protein (from cell debris sample). a). IPTG concentration optimization for H<sub>6</sub>-TEV-bFGF expression and b). IPTG concentration optimization for H<sub>6</sub>-TEV-(GAGAGS)<sub>6</sub>-bFGF.

#### 4.8.2.1 H<sub>6</sub>-TEV-bFGF purification

After H<sub>6</sub>-TEV-bFGF large scale production, soluble protein was extracted and kept the supernatant for purify step. H<sub>6</sub>-TEV-bFGF was purified using Ni-NTA agarose column. The result of the first purification step was detected by Coomassie blue staining Fig. 18. Then, TEV protease was added to MBP-H<sub>6</sub>-TEV-bFGF fraction for digested at TEV site. After that, the digestive peptide was purified again with Ni-NTA agarose column (Fig 18).

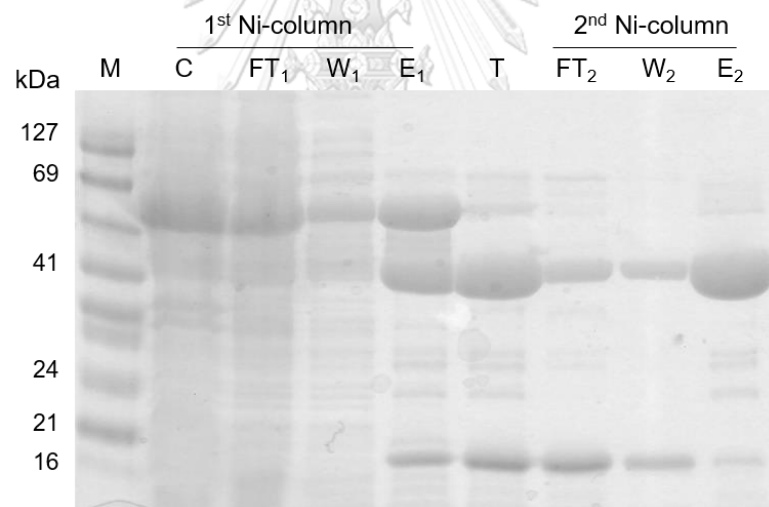


Figure 18: The histidine tag-containing TEV-bFGF purification. M = protein marker. The 1<sup>st</sup> Ni-column; C = protein input solution, FT<sub>1</sub> = protein unbonded solution, W<sub>1</sub> = protein in 25 mM imidazole-containing buffer washed fraction, E<sub>1</sub> = MBP-H<sub>6</sub>-TEV-bFGF in 250 imidazole buffer. T = TEV protease cut check fraction. The 2<sup>nd</sup> Ni-column; FT<sub>2</sub> = bFGF, W<sub>2</sub> = bFGF in 25 mM imidazole-containing buffer washed fraction, E<sub>2</sub> = MBP-H<sub>6</sub> in 250 imidazole buffer

The flowthrough fraction of bFGF peptide in 2<sup>nd</sup> Ni-NTA agarose column was purified with ion-exchange chromatography with SP column for remove TEV protease. The peptide purification result is shown in Fig 19. In this case, the E4-E7 fractions of eluted bFGF were selected. After concentration using centrifugal filter, the peptide concentration was determined using  $A_{280}$  following by Beer's law and shown the concentration in table 16.

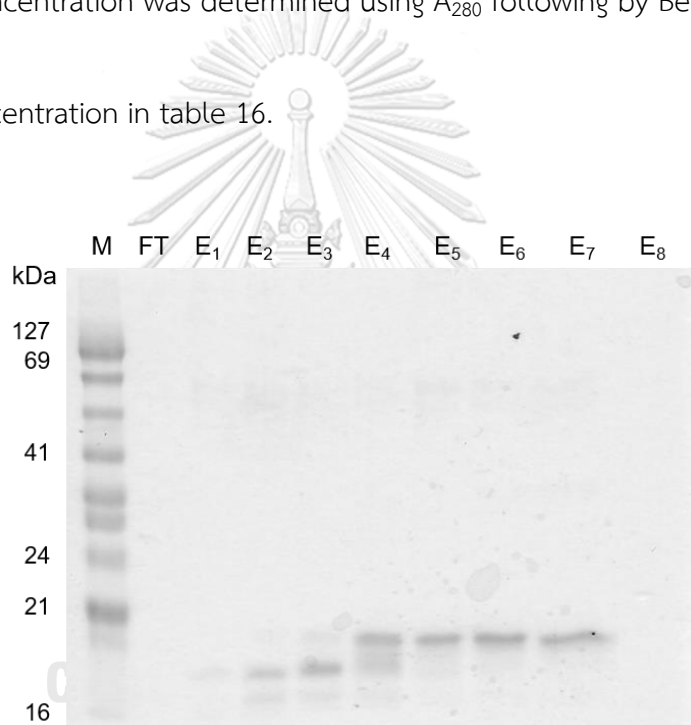


Figure 19: The bFGF purification by ion-exchange chromatography. M = protein marker, FT = protein unbonded solution, E<sub>1</sub>-E<sub>8</sub> = eluted protein fraction from 0 mM – 1 M of NaCl in 20 mM Tris, pH 7.5 buffer.

#### 4.8.2.2 H<sub>6</sub>-TEV-(GAGAGS)<sub>6</sub>-bFGF purification

After H<sub>6</sub>-TEV-(GAGAGS)<sub>6</sub>-bFGF large scale production, soluble protein was extracted and the supernatant kept for purification. H<sub>6</sub>-TEV-(GAGAGS)<sub>6</sub>-bFGF was purified using Ni-NTA agarose column. Then, TEV protease was added to MBP-H<sub>6</sub>-TEV-(GAGAGS)<sub>6</sub>-bFGF fraction for digested at TEV site. After that, the digestive peptide was purified again with Ni-NTA agarose column (Fig 20).

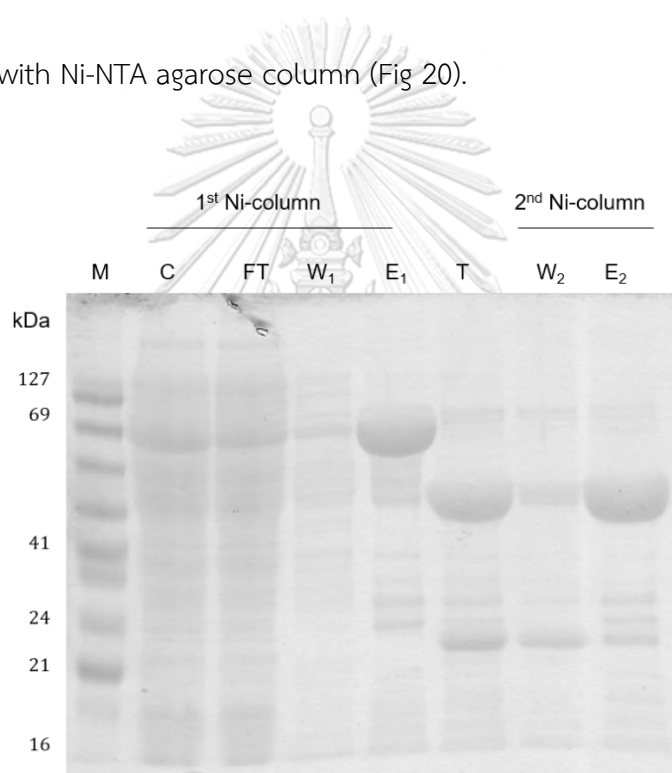


Figure 20: The histidine tag-containing TEV-(GAGAGS)<sub>6</sub>-bFGF purification. M = protein marker. The 1<sup>st</sup> Ni-column; C = protein input solution, FT = protein unbonded solution, W<sub>1</sub> = protein in 25 mM imidazole-containing buffer washed fraction, E<sub>1</sub> = MBP-H<sub>6</sub>-TEV-(GAGAGS)<sub>6</sub>-bFGF in 250 imidazole buffer. T = TEV protease cut check fraction. The 2<sup>nd</sup> Ni-column; W<sub>2</sub> = (GAGAGS)<sub>6</sub>-bFGF in 25 mM imidazole-containing buffer washed fraction, E<sub>2</sub> = MBP-H<sub>6</sub> in 250 imidazole buffer.

The flow-through fraction of H6-TEV-(GAGAGS)<sub>6</sub>-bFGF peptide from the 2<sup>nd</sup> Ni-NTA agarose column purification was further purified with ion-exchange chromatography. The peptide purification result is shown in Fig 21. In this case, the E3-E5 fractions of eluted H6-TEV-(GAGAGS)<sub>6</sub>-bFGF were selected. After concentration using centrifugal filter, the peptide concentration was determined using  $A_{280}$  following by Beer's law and shown the concentration in table 16.

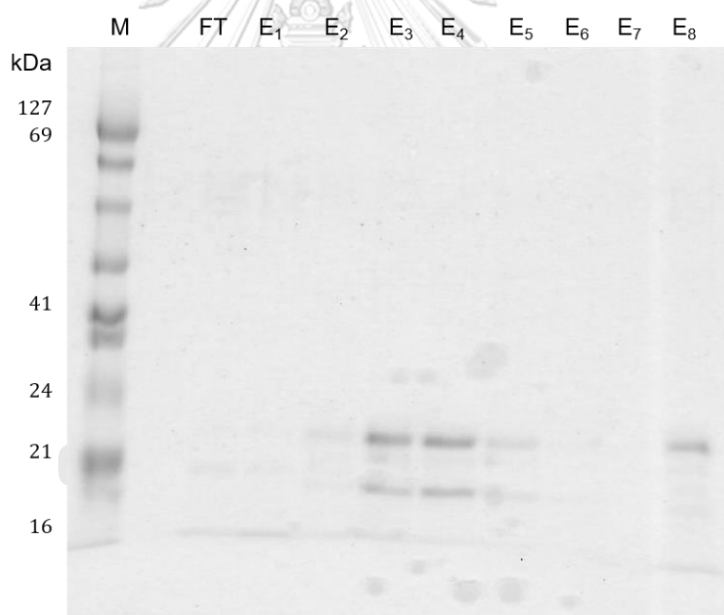


Figure 21: The (GAGAGS)<sub>6</sub>-bFGF purification by ion-exchange chromatography. M = protein marker, FT = protein unbonded solution, E<sub>1</sub>-E<sub>8</sub> = eluted protein fraction from 0 mM – 1 M of NaCl in 20 mM Tris, pH 7.5 buffer.

*Table 13: The concentration of bFGF recombinant peptide*

Peptide	$A_{280}$	$\epsilon$ ( $M^{-1} \text{ cm}^{-1}$ )	Concentration (mg/ml)
bFGF from pET28b	0.604	15,930	0.65
bFGF from pMALc5x	0.979	15,930	1.10
(GAGAGS) <sub>6</sub> -bFGF from pMALc5x	1.02	15,930	1.29

#### 4.9. Application of bFGF, bFGF from pMALc5x and (GAGAGS)<sub>6</sub>-bFGF peptide on tissue engineering

##### 4.9.1 Optimization of bFGF, bFGF from pMALc5x and (GAGAGS)<sub>6</sub>-bFGF concentration for cell proliferation.

Before applied these peptides on tissue engineering, The optimization of peptides concentration for cell survival was determined. NIH-3T3 proliferation ( $10^3$  cells/ml) was determined by various concentration of peptides from 0 – 100 ng/ml. After 24 hour of cell culture, MTT assay was performed for elucidate the cell proliferation. The result, shown in Fig 22, explained that 100 ng/ml of all peptides had the highest of absorbance of 570 nm light and lower absorption at 1 and 10

ng/ml peptide concentration. The absorption value in these results can elucidated that all peptides can induced NIH-3T3 proliferation and showed the function of native form.

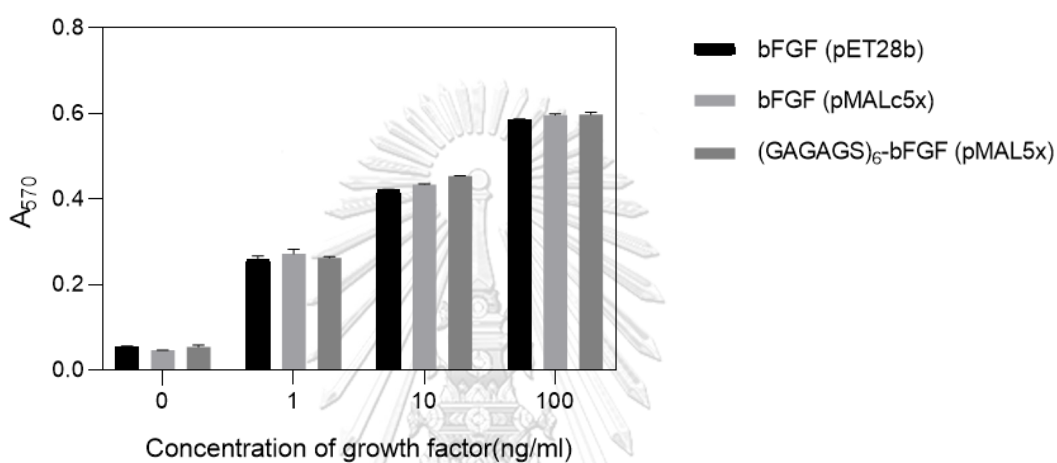


Figure 22: Concentration optimization of three types bFGF peptide on NIH-3T3 proliferation detected by MTT assay.

#### 4.9.2 *In vitro* bFGF release determined by cell proliferation.

To explore the repeat unit of SF on CRS in tissue engineering application, Production of SF, SF/bFGF, SF/bFGF<sub>(pMALC5x)</sub>, and SF/(GAGAGS)<sub>6</sub>-bFGF hydrogel were performed and cut these hydrogels into cubic shape. After that, NIH-3T3 were cultured in 6-well plates containing 0.1% FBS culture media and each well had four hydrogels cubic that had 1 ng/ml of peptide. The metabolic activity of cell culture

with SF/bFGF and SF/bFGF<sub>(pMALC5x)</sub> rapidly increased of A<sub>570</sub> in 8 days and stable over the time course of 16 days culture periods. Interestingly, the metabolic activity value of cell culture with SF/(GAGAGS)<sub>6</sub>-bFGF hydrogel gradually increased in day 10 and stable over the time course of culture periods Fig 23. These results illustrated that increasing repeat unit of SF could control bFGF release in first linear and sustained release for support NIH-3T3 proliferation.

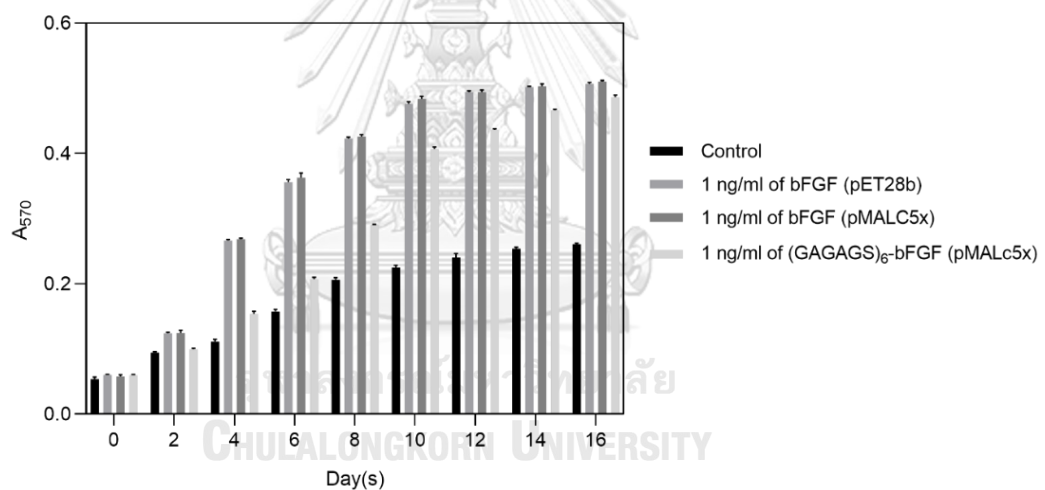


Figure 23: In vitro of bFGF release from SF hydrogel on NIH-3T3 proliferation detected by cellular activity assay (MTT)



## CHAPTER V

### DISCUSSION AND CONCLUSION

Many medical drugs are conventional (“free”) drug delivery systems (DDS) for medical treatment, but these systems are hardly controlled processes because the drug release rate is difficult to manage. These effects can cause many disadvantages such as poor solubility, tissue damage, unfavorable pharmacokinetics, and lack of selectivity for target tissue. Control release system (CRS) is an important class of DDS for improving drug release (Tibbitt et al., 2016). Nowadays, the natural polymer CRS material has been developed and designed as a vehicle not only for carrier a drug and sustain release at desirable concentration and correct target but also there can protect the biological function of the protein drug (Tong et al., 2020). Silk fibroin (SF) is the most popular natural polymer used in CRS (Wenk et al., 2011). SF had various good properties such as biocompatibility, mechanical strength, and biocompatibility and showed an excellent choice for the delivery of bioactive molecules (Koh et al., 2015). In the past, there have many studies that used conventional SF-based

hydrogel-controlled drug release and maintained bioactive compound activity, but these molecules release from SF hydrogel in a non-linear manner (de Moraes et al., 2015). To solve these problems, SF/copolymer composite hydrogel was used to improve the release profile because the hydrophobic and hydrophilic of copolymer could help to sustain drug release, but this system is non-linear drug release manner (Zhong et al., 2015).

The primary structure of SF protein contains two polypeptide chains hydrophobic heavy chain and a hydrophilic light chain that has a molecular weight of around 200 – 350 kDa. The amino acid sequence of the hydrophobic heavy chain has a repetitive block and the sequence GAGAGS repeat unit shows the highest repetitive unit in this chain. The repetitive unit of hydrophobic block folds and form  $\beta$ -sheet crystalline structure via hydrophobic bonds, van der Waals force, and hydrophobic interaction (Zhou et al., 2001). These crystalline structures of SF can help control drug release profiles. From the knowledge and advantage properties of repetitive unit sequence in natural protein, several researchers have tried to synthesize repeating units of protein that mimic the known amino acid sequence in natural protein

structure. For example, Collagen mimetic peptide or CMPs has synthesized 7 Gly-X-Y units and coupled to a growth factor that mimics the natural collagen. CMPs can adhere to loops or interrupt the triple helix of natural collagen and sustain the release of growth factors from mimic CMPs in wound healing (Chattopadhyay et al., 2012). Another research was on the recombinant spider silk protein eADF4 (C16) that mimicked the 16 repeating unit amino acid sequence of spider silk protein. The mimic spider silk can be prepared into various forms of drug carrier and has shown that spider silk was the potential to sustain the drug release system (Spiess et al., 2010).

In this study, the repeating unit of silk fibroin (GAGAGS) fused with GFP amino acid sequence was synthesized from zero of GAGAGS to seven of GAGAGS and purified into pure peptides by chromatography methods. These recombinant peptides had the function that was detected by its green fluorescent color of GFP peptide shown in Fig 4.2b. The effect of the repeat unit of SF on CRS was determined by in vitro release. The release profile of GFP from SF hydrogel showed GFP release accumulation detected by its GFP absorbance at 395 nm light (Prasher et

al., 1992). A release accumulation at equilibrium of GFP release was detected at 10 minutes. The release rate of GFP was subsequently decreased by increasing the GAGAGS unit of SF. Surprisingly, the highest [(GAGAGS)<sub>7</sub>-GFP] in SF hydrogel showed the slowest release rate and GFP accumulation at equilibrium occurred in 96 hours. Not only increasing the GAGAGS unit of SF can reduce the burst release effect and control the protein drug release profile but also all repeat units can maintain and sustain release for up to one week. The result can explain that the recombinant (GAGAGS)<sub>n</sub>-GFP peptides had hydrophobic interaction with the repeat unit of the SF hydrogel scaffold. This evidence showed that increasing the GAGAGS unit can increase interaction between GAGAGS mimic peptide and nature GAGAGS scaffold that controlled the release rate and sustained release profile (Koh et al., 2015). The effect of (GAGAGS)<sub>n</sub>-GFP was showed in the gelation time of SF hydrogel (Fig. 4.3). The larger GAGAGS units can induce gel formation or reduced the gelation time of SF hydrogel. The hydrogel formation was dealt with secondary structure change of SF protein. The SF structure in SF solution changed from a disordered state to  $\beta$ -sheet conformation in a hydrogel state (Matsumoto et al., 2006). This

result explained that the higher GAGAGS unit can change the structure from disorder to crystalline is faster and depend on the increase of hydrophobic force too. In addition, the increasing unit of  $(\text{GAGAGS})_n\text{-GFP}$  can reduce the degradation rate of SF hydrogel. The remaining SF/ $(\text{GAGAGS})_n = 5,6,7\text{-GFP}$  hydrogel weight showed an upper 50% at the end of the experiment (Day 30). This result can exhibit that the GFP release profile from SF hydrogel may depend on degradation mechanism and the SF hydrogel with a larger unit of SF can help to prolong the scaffold for tissue regeneration (Lu et al., 2011).

To find the reason about the GFP release process, the structure analysis of repeating unit tagged GFP peptide loaded hydrogel by FTIR and XRD revealed that the repeat unit-tagged GFP peptide can increase the crystalline  $\beta$ -sheet fraction in the hydrogel. Therefore, the in vitro release of GFP was not only dependent on the secondary structure of SF but this process also involves in intermolecular force between repeat unit of mimicked peptide and SR unit in SF hydrogel.

Finally, the benefit of repeat unit SF was applied in tissue engineering (Kasaju & Bora, 2012). The recombinant of bFGF and (GAGAGS)<sub>6</sub>-bFGF was produced. These recombinant peptides had function because their induced cell line proliferation detected by metabolic activity (MTT assay) (Bikfalvi et al., 1997). Subsequently, the application of recombinant peptide on cellular function was performed. The NIH-3T3 was slightly grow when incubated with (SR)<sub>6</sub>-bFGF while was rapidly proliferated with bFGF. The larger of SR tagged growth factor could be reduce the burst release effect and controlled release of bFGF from scaffold. This advantage can be applied in tissue engineering for medical proposes.

### Conclusions

The repeating unit of SF tagged protein drug mimic peptide does not alter the function of the tagged protein. In addition, increasing the repeat unit can reduced the gel formation. The tagged protein can be attached into SF hydrogel possibility by interacting with crystalline  $\beta$ -sheets structure. The interaction between repeating unit mimic peptide and SF scaffold leads to the sustained release of the protein drug and

slower degradation of the hydrogel. Moreover, increasing the repeat unit-tagged growth factor can control the growth factor release profile. The result in this dissertation provides evidence that genetic engineering of the sequence and length of repeat unit mimic peptide allows control the release rate and degradation rate to use in diverse application.







## Culture media for bacteria

## LB

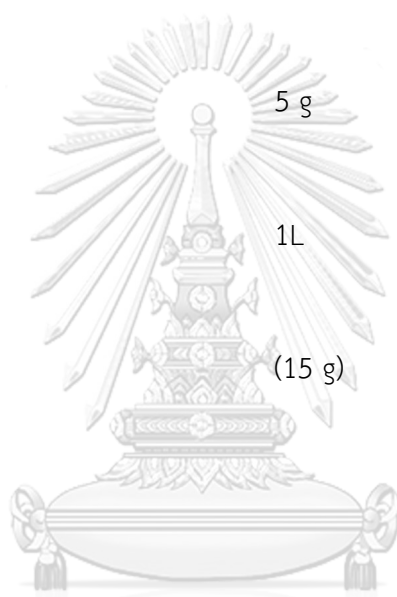
Tryptone 10 g

Yeast extract 5 g

NaCl 5 g

Water 1L

(Agar) (15 g)



## SOB

จุฬาลงกรณ์มหาวิทยาลัย  
CHULALONGKORN UNIVERSITY

Tryptone 20 g

Yeast extract 5 g

NaCl 0.5 g

1 M KCl 2.5 ml

1 M MgCl<sub>2</sub> 10 ml

1 M MgSO<sub>4</sub> 10 ml

Water To 1 L

(SOC = SOB + 20 mM Glucose)

**Terrific broth**

Tryptone 12 g

Yeast extract 24 g

Glycerol 4 ml

Water To 1 L



## CCMB80 buffer pH 6.4

KOAc 0.981 g

CaCl<sub>2</sub> 11.8 g

MgCl<sub>2</sub> 2.03 g

Glycerol 100 ml

MnCl<sub>2</sub> (added later) 1.98 g

Water To 1 L

## TSB buffer

Tryptone 10 g

Yeast extract 5 g

NaCl 5.84 g

PEG3350 100 g



DMSO	50 ml
MgCl <sub>2</sub>	0.95 g
MgSO <sub>4</sub>	1.20 g

Phosphate buffer

KH <sub>2</sub> PO <sub>4</sub>	23.14 g
K <sub>2</sub> HPO <sub>4</sub>	135.41 g
Water	1 L



Antibiotics

Table 14: Antibiotics stock concentration

Antibiotics	1000x stock concentration	solvent
Ampicillin	100 mg/ml	Water
Kanamycin	50 mg/ml	Water
IPTG	23.83 mg/ml	Water

## Buffers

### 6x SDS Sample buffer

SDS	1.2 g
Glycerol	4.7 ml
0.5 M Tris pH 6.8	1.2 ml
Bromophenol blue	6 mg
DTT	0.93 g
Water	2.1 ml



จุฬาลงกรณ์มหาวิทยาลัย  
CHULALONGKORN UNIVERSITY

### 10x Running buffer

Tris	30.3 g
Glycine	144.0 g
SDS	10.0 g

Water 1 L

### 50x TAE

Tris 242 g

Acetic acid 57.1 ml

500 mM EDTA, pH 8.0 100 ml

Water To 1 L



### 12% Resolving gel

Water 3.4 ml

Acrylamide/Bis 37:5:1 30%T, 2.67%C 4.0 ml

1.5 M Tris pH 8.8 2.1 ml

10% SDS 0.1 ml

TEMED 5  $\mu$ l

10% Ammonium persulfate (fresh) 50  $\mu$ l

(total volume = 10 ml for 2 gels)

### 6% Stacking gel

Water 2.7 ml

Acrylamide/Bis 37:5:1 30%T, 2.67% C 1.0 ml

0.5 M Tris pH 6.8 1.25 ml

10% SDS 50  $\mu$ l

TEMED 5  $\mu$ l

10% Ammonium persulfate (fresh) 25  $\mu$ l

(total volume = 5 ml for 2 gels)



**Coomassie Brilliant blue staining**

Coomassie Brilliant Blue (R-250)	1 g
Water	400 ml
Methanol	500 ml
Acetic acid	100 ml

**Coomassie Brilliant blue destaining**

Water	500 ml
Methanol	400 ml
Acetic acid	100 ml



จุฬาลงกรณ์มหาวิทยาลัย  
CHULALONGKORN UNIVERSITY

**Bradford reagent**

Coomassie Brilliant Blue (G-250)	100 mg
----------------------------------	--------



95% ethanol	50 ml
85% phosphoric acid	100 ml
Water	850 ml

### 1% Agarose gel

Agarose	0.5 g
TAE	50 ml
HydraGreen™ Safe DNA Dye	1 $\mu$ l



## Competent cell preparation

### *E. coli* DH10 $\beta$

*E. coli* DH10 $\beta$  was grown in 100 ml of SOB media at 30°C until OD<sub>600</sub> reached 0.3. The cells were then collected by centrifugation at 6,000 xg, 4°C, for 5 minutes. After discarding the supernatant, the pellet was resuspended in 30 ml of ice-cold fresh CCMB80 buffer. After 20 minutes of incubation on ice, the cells were pelleted and resuspended in 0.04 culture volume of ice-cold CCMB80. Finally, the competent cells were aliquoted and snap freeze in liquid nitrogen and stored at -80°C.

### *E. coli* Tuner(DE3)

*E. coli* Tuner(DE3) was grown in 100 ml of LB media at 37°C until OD<sub>600</sub> reached 0.6. The cells were collected by centrifugation at 6,000 xg, 4°C, for 5 minutes. The pellet was then resuspended in 0.05 culture volume of ice-cold TSB buffer for 10 minutes. The competent cells were aliquoted and snap freeze in liquid nitrogen and stored at -80°C.

### Determining of protein concentration by Bradford assay

BSA standard concentration in the range of 0 – 100  $\mu\text{g/ml}$  (100  $\mu\text{l}$ ) were added into a cuvette as 3 sets. The protein sample (100  $\mu\text{l}$ ) and buffer (100  $\mu\text{l}$ ) as blank were added into cuvette as 3 sets. The Bradford reagent was then added (900  $\mu\text{l}$ ) into each cuvette of BSA standard, blank, and protein sample. The reactions were incubated in the dark at room temperature, for 10 minutes. Absorbance at 595 nm was then measured by spectrophotometer. Finally, the BSA standard curve was plotted by Microsoft Excel. The protein sample concentration was determined using  $A_{595}$  and linear regression equation obtained from linear fit of the BSA standard curve.

## Standard curve

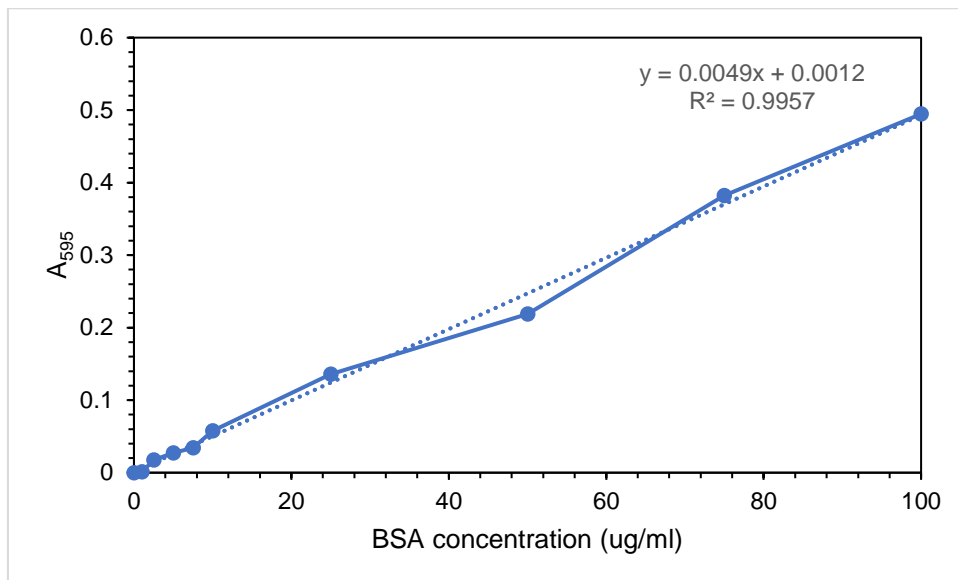


Figure 24: Standard curve for  $(GAGAGS)_n$ -GFP

Mammalian cell culture

Mammalian cell culture media

- Complete cell culture media

DMEM media high glucose                      250 ml

Fetal Bovine Serum                                25 ml

Penicillin-Streptomycin                        2.5 ml

- Non-complete cell culture media

DMEM media high glucose                      250 ml

Fetal Bovine Serum                              0.25 ml

Penicillin-Streptomycin                      2.5 ml

### Mammalian cell counting

NIH-3T3 mammalian cell lines were required knowledge of cell concentration before seeding. The mammalian cell suspension was sampled (20  $\mu$ l) was applied onto a hemacytometer. The cells were counted in all 8 squares, then the cell concentration was calculated using the following formula;

$$\text{Cells concentration } \left( \frac{\text{cells}}{\text{ml}} \right) = \text{total counted cells} \times \frac{10^4}{\text{number of squares}}$$

## MTT Assay

- MTT solution

MTT 100 mg

Water 10 ml

- MTT solvent

HCl 12.37  $\mu$ l



## REFERENCES

- Akl, M., Hm, A.-E., & Em, A. B. (2018). Poly (Ethylene-Co-Vinyl Acetate) Blends for Controlled Drug Release. *American Journal of Advanced Drug Delivery*, 6.
- Altman, G. H., Diaz, F., Jakuba, C., Calabro, T., Horan, R. L., Chen, J., Lu, H., Richmond, J., & Kaplan, D. L. (2003). Silk-based biomaterials. *Biomaterials*, 24(3), 401-416.  
[https://doi.org/https://doi.org/10.1016/S0142-9612\(02\)00353-8](https://doi.org/https://doi.org/10.1016/S0142-9612(02)00353-8)
- Bayraktar, O., Malay, Ö., Özgarip, Y., & Batıgün, A. (2005). Silk fibroin as a novel coating material for controlled release of theophylline. *European Journal of Pharmaceutics and Biopharmaceutics*, 60(3), 373-381.  
<https://doi.org/https://doi.org/10.1016/j.ejpb.2005.02.002>
- Bikfalvi, A., Klein, S., Pintucci, G., & Rifkin, D. B. (1997). Biological Roles of Fibroblast Growth Factor-2\*. *Endocrine Reviews*, 18(1), 26-45.  
<https://doi.org/10.1210/edrv.18.1.0292>
- Brandi, M. L., & Collin-Osdoby, P. (2006). Vascular Biology and the Skeleton. *Journal of Bone and Mineral Research*, 21(2), 183-192.  
<https://doi.org/https://doi.org/10.1359/JBMR.050917>
- Chattopadhyay, S., Murphy, C. J., McAnulty, J. F., & Raines, R. T. (2012). Peptides that anneal to natural collagen in vitro and ex vivo [10.1039/C2OB25190F]. *Organic & Biomolecular Chemistry*, 10(30), 5892-5897. <https://doi.org/10.1039/C2OB25190F>
- Choi, M., Choi, D., & Hong, J. (2018). Multilayered Controlled Release Silk Fibroin Nanofilm by Manipulating Secondary Structure. *Biomacromolecules*, 19(7), 3096-3103. <https://doi.org/10.1021/acs.biomac.8b00687>
- Coburn, J., Harris, J., Zakharov, A. D., Poirier, J., Ikegaki, N., Kajdacsy-Balla, A., Pilichowska, M., Lyubimov, A. V., Shimada, H., Kaplan, D. L., & Chiu, B. (2017). Implantable chemotherapy-loaded silk protein materials for neuroblastoma treatment. *International Journal of Cancer*, 140(3), 726-735.  
<https://doi.org/https://doi.org/10.1002/ijc.30479>
- Coburn, J. M., Harris, J., Cunningham, R., Zeki, J., Kaplan, D. L., & Chiu, B. (2017). Manipulation of variables in local controlled release vincristine treatment in



neuroblastoma. *J Pediatr Surg*, 52(12), 2061-2065.

<https://doi.org/10.1016/j.jpedsurg.2017.08.028>

de Moraes, M. A., Albrecht Mahl, C. R., Ferreira Silva, M., & Beppu, M. M. (2015).

Formation of silk fibroin hydrogel and evaluation of its drug release profile.

*Journal of Applied Polymer Science*, 132(15).

<https://doi.org/https://doi.org/10.1002/app.41802>

Dinerman, A. A., Cappello, J., Ghandehari, H., & Hoag, S. W. (2002). Solute diffusion in genetically engineered silk-elastinlike protein polymer hydrogels. *Journal of Controlled Release*, 82(2), 277-287.

[https://doi.org/https://doi.org/10.1016/S0168-3659\(02\)00134-7](https://doi.org/https://doi.org/10.1016/S0168-3659(02)00134-7)

Elia, R., Newhide, D. R., Pedevillano, P. D., Reiss, G. R., Firpo, M. A., Hsu, E. W., Kaplan, D.

L., Prestwich, G. D., & Peattie, R. A. (2013). Silk-hyaluronan-based composite hydrogels: a novel, securable vehicle for drug delivery. *J Biomater Appl*, 27(6),

749-762. <https://doi.org/10.1177/0885328211424516>

Elzoghby, A. O., Samy, W. M., & Elgindy, N. A. (2012). Albumin-based nanoparticles as potential controlled release drug delivery systems. *Journal of Controlled Release*, 157(2), 168-182.

<https://doi.org/https://doi.org/10.1016/j.jconrel.2011.07.031>

Fang, J. Y., Chen, J. P., Leu, Y. L., & Wang, H. Y. (2006). Characterization and evaluation of silk protein hydrogels for drug delivery. *Chem Pharm Bull (Tokyo)*, 54(2), 156-162. <https://doi.org/10.1248/cpb.54.156>

Fenton, O. S., Olafson, K. N., Pillai, P. S., Mitchell, M. J., & Langer, R. (2018). Advances in Biomaterials for Drug Delivery. *Advanced Materials*, 30(29), 1705328.

<https://doi.org/https://doi.org/10.1002/adma.201705328>

Freiberg, S., & Zhu, X. X. (2004). Polymer microspheres for controlled drug release.

*International Journal of Pharmaceutics*, 282(1), 1-18.

<https://doi.org/https://doi.org/10.1016/j.ijpharm.2004.04.013>

Galateanu, B., Hudita, A., Zaharia, C., Bunea, M.-C., Vasile, E., Buga, M.-R., & Costache, M.

(2019). Silk-Based Hydrogels for Biomedical Applications. In M. I. H. Mondal (Ed.), *Cellulose-Based Superabsorbent Hydrogels* (pp. 1791-1817). Springer International Publishing.

[https://doi.org/10.1007/978-3-319-77830-3\\_59](https://doi.org/10.1007/978-3-319-77830-3_59)

- Gospodarowicz, D. (1974). Localisation of a fibroblast growth factor and its effect alone and with hydrocortisone on 3T3 cell growth. *Nature*, 249(5453), 123-127.  
<https://doi.org/10.1038/249123a0>
- Guziewicz, N., Best, A., Perez-Ramirez, B., & Kaplan, D. L. (2011). Lyophilized silk fibroin hydrogels for the sustained local delivery of therapeutic monoclonal antibodies. *Biomaterials*, 32(10), 2642-2650.  
<https://doi.org/https://doi.org/10.1016/j.biomaterials.2010.12.023>
- Hamid Akash, M. S., Rehman, K., & Chen, S. (2015). Natural and Synthetic Polymers as Drug Carriers for Delivery of Therapeutic Proteins. *Polymer Reviews*, 55(3), 371-406. <https://doi.org/10.1080/15583724.2014.995806>
- Hoffman, A. S. (2008). The origins and evolution of “controlled” drug delivery systems. *Journal of Controlled Release*, 132(3), 153-163.  
<https://doi.org/https://doi.org/10.1016/j.jconrel.2008.08.012>
- Hu, L., Sun, Y., & Wu, Y. (2013). Advances in chitosan-based drug delivery vehicles [10.1039/C3NR00338H]. *Nanoscale*, 5(8), 3103-3111.  
<https://doi.org/10.1039/C3NR00338H>
- Humenik, M., Mohrand, M., & Scheibel, T. (2018). Self-Assembly of Spider Silk-Fusion Proteins Comprising Enzymatic and Fluorescence Activity. *Bioconjugate Chemistry*, 29(4), 898-904. <https://doi.org/10.1021/acs.bioconjchem.7b00759>
- Inoue, S., Tanaka, K., Arisaka, F., Kimura, S., Ohtomo, K., & Mizuno, S. (2000). Silk Fibroin of *Bombyx mori* Is Secreted, Assembling a High Molecular Mass Elementary Unit Consisting of H-chain, L-chain, and P25, with a 6:6:1 Molar Ratio \*. *Journal of Biological Chemistry*, 275(51), 40517-40528.  
<https://doi.org/10.1074/jbc.M006897200>
- Kasoju, N., & Bora, U. (2012). Silk Fibroin in Tissue Engineering. *Advanced Healthcare Materials*, 1(4), 393-412. <https://doi.org/https://doi.org/10.1002/adhm.201200097>
- Kim, J. K., Kim, H. J., Chung, J.-Y., Lee, J.-H., Young, S.-B., & Kim, Y.-H. (2014). Natural and synthetic biomaterials for controlled drug delivery. *Archives of Pharmacal Research*, 37(1), 60-68. <https://doi.org/10.1007/s12272-013-0280-6>
- Kirker-Head, C. A. (2000). Potential applications and delivery strategies for bone morphogenetic proteins. *Advanced Drug Delivery Reviews*, 43(1), 65-92.

- [https://doi.org/https://doi.org/10.1016/S0169-409X\(00\)00078-8](https://doi.org/https://doi.org/10.1016/S0169-409X(00)00078-8)
- Koh, L.-D., Cheng, Y., Teng, C.-P., Khin, Y.-W., Loh, X.-J., Tee, S.-Y., Low, M., Ye, E., Yu, H.-D., Zhang, Y.-W., & Han, M.-Y. (2015). Structures, mechanical properties and applications of silk fibroin materials. *Progress in Polymer Science*, *46*, 86-110. <https://doi.org/https://doi.org/10.1016/j.progpolymsci.2015.02.001>
- Lammel, A., Schwab, M., Hofer, M., Winter, G., & Scheibel, T. (2011). Recombinant spider silk particles as drug delivery vehicles. *Biomaterials*, *32*(8), 2233-2240. <https://doi.org/https://doi.org/10.1016/j.biomaterials.2010.11.060>
- Lu, Q., Zhang, B., Li, M., Zuo, B., Kaplan, D. L., Huang, Y., & Zhu, H. (2011). Degradation Mechanism and Control of Silk Fibroin. *Biomacromolecules*, *12*(4), 1080-1086. <https://doi.org/10.1021/bm101422j>
- Mandal, B. B., Kapoor, S., & Kundu, S. C. (2009). Silk fibroin/polyacrylamide semi-interpenetrating network hydrogels for controlled drug release. *Biomaterials*, *30*(14), 2826-2836. <https://doi.org/https://doi.org/10.1016/j.biomaterials.2009.01.040>
- Martino, M. M., Briquez, P. S., Maruyama, K., & Hubbell, J. A. (2015). Extracellular matrix-inspired growth factor delivery systems for bone regeneration. *Advanced Drug Delivery Reviews*, *94*, 41-52. <https://doi.org/https://doi.org/10.1016/j.addr.2015.04.007>
- Matsumoto, A., Chen, J., Collette, A. L., Kim, U.-J., Altman, G. H., Cebe, P., & Kaplan, D. L. (2006). Mechanisms of Silk Fibroin Sol-Gel Transitions. *The Journal of Physical Chemistry B*, *110*(43), 21630-21638. <https://doi.org/10.1021/jp056350v>
- Megeed, Z., Cappello, J., & Ghandehari, H. (2002). Controlled Release of Plasmid DNA from a Genetically Engineered Silk-Elastinlike Hydrogel. *Pharmaceutical Research*, *19*(7), 954-959. <https://doi.org/10.1023/A:1016406120288>
- Mehtani, D., Seth, A., Sharma, P., Maheshwari, N., Kapoor, D., Shrivastava, S. K., & Tekade, R. K. (2019). Chapter 4 - Biomaterials for Sustained and Controlled Delivery of Small Drug Molecules. In R. K. Tekade (Ed.), *Biomaterials and Bionanotechnology* (pp. 89-152). Academic Press. <https://doi.org/https://doi.org/10.1016/B978-0-12-814427-5.00004-4>
- Nguyen, T. P., Nguyen, Q. V., Nguyen, V.-H., Le, T.-H., Huynh, V. Q. N., Vo, D.-V. N., Trinh,

- Q. T., Kim, S. Y., & Le, Q. V. (2019). Silk Fibroin-Based Biomaterials for Biomedical Applications: A Review. *Polymers*, 11(12), 1933. <https://www.mdpi.com/2073-4360/11/12/1933>
- Nugent, M. A., & Iozzo, R. V. (2000). Fibroblast growth factor-2. *The International Journal of Biochemistry & Cell Biology*, 32(2), 115-120. [https://doi.org/https://doi.org/10.1016/S1357-2725\(99\)00123-5](https://doi.org/https://doi.org/10.1016/S1357-2725(99)00123-5)
- Numata, K., Mieszawska-Czajkowska, A. J., Kvenvold, L. A., & Kaplan, D. L. (2012). Silk-Based Nanocomplexes with Tumor-Homing Peptides for Tumor-Specific Gene Delivery. *Macromolecular Bioscience*, 12(1), 75-82. <https://doi.org/https://doi.org/10.1002/mabi.201100274>
- Panduranga Rao, K. (1996). Recent developments of collagen-based materials for medical applications and drug delivery systems. *Journal of Biomaterials Science, Polymer Edition*, 7(7), 623-645. <https://doi.org/10.1163/156856295X00526>
- Porter, D., & Vollrath, F. (2009). Silk as a Biomimetic Ideal for Structural Polymers. *Advanced Materials*, 21(4), 487-492. <https://doi.org/https://doi.org/10.1002/adma.200801332>
- Prasher, D. C., Eckenrode, V. K., Ward, W. W., Prendergast, F. G., & Cormier, M. J. (1992). Primary structure of the *Aequorea victoria* green-fluorescent protein. *Gene*, 111(2), 229-233. [https://doi.org/https://doi.org/10.1016/0378-1119\(92\)90691-H](https://doi.org/https://doi.org/10.1016/0378-1119(92)90691-H)
- Pritchard, E. M., Valentin, T., Panilaitis, B., Omenetto, F., & Kaplan, D. L. (2013). Antibiotic-Releasing Silk Biomaterials for Infection Prevention and Treatment. *Advanced Functional Materials*, 23(7), 854-861. <https://doi.org/https://doi.org/10.1002/adfm.201201636>
- Qi, Y., Wang, H., Wei, K., Yang, Y., Zheng, R.-Y., Kim, I. S., & Zhang, K.-Q. (2017). A Review of Structure Construction of Silk Fibroin Biomaterials from Single Structures to Multi-Level Structures. *International Journal of Molecular Sciences*, 18(3), 237. <https://www.mdpi.com/1422-0067/18/3/237>
- Rujiravanit, R., Kruaykitanon, S., Jamieson, A. M., & Tokura, S. (2003). Preparation of Crosslinked Chitosan/Silk Fibroin Blend Films for Drug Delivery System. *Macromolecular Bioscience*, 3(10), 604-611.

- <https://doi.org/https://doi.org/10.1002/mabi.200300027>
- Spiess, K., Lammel, A., & Scheibel, T. (2010). Recombinant Spider Silk Proteins for Applications in Biomaterials. *Macromolecular Bioscience*, 10(9), 998-1007. <https://doi.org/https://doi.org/10.1002/mabi.201000071>
- Stinson, J. A., Raja, W. K., Lee, S., Kim, H. B., Diwan, I., Tutunjian, S., Panilaitis, B., Omenetto, F. G., Tzipori, S., & Kaplan, D. L. (2017). Silk Fibroin Microneedles for Transdermal Vaccine Delivery. *ACS Biomaterials Science & Engineering*, 3(3), 360-369. <https://doi.org/10.1021/acsbiomaterials.6b00515>
- Sung, Y. K., & Kim, S. W. (2020). Recent advances in polymeric drug delivery systems. *Biomaterials Research*, 24(1), 12. <https://doi.org/10.1186/s40824-020-00190-7>
- Tabata, Y. (2003). Tissue Regeneration Based on Growth Factor Release. *Tissue Engineering*, 9(supplement 1), 5-15. <https://doi.org/10.1089/10763270360696941>
- Tibbitt, M. W., Dahlman, J. E., & Langer, R. (2016). Emerging Frontiers in Drug Delivery. *Journal of the American Chemical Society*, 138(3), 704-717. <https://doi.org/10.1021/jacs.5b09974>
- Tomeh, M. A., Hadianamrei, R., & Zhao, X. (2019). Silk Fibroin as a Functional Biomaterial for Drug and Gene Delivery. *Pharmaceutics*, 11(10), 494. <https://www.mdpi.com/1999-4923/11/10/494>
- Tong, X., Pan, W., Su, T., Zhang, M., Dong, W., & Qi, X. (2020). Recent advances in natural polymer-based drug delivery systems. *Reactive and Functional Polymers*, 148, 104501. <https://doi.org/https://doi.org/10.1016/j.reactfunctpolym.2020.104501>
- Tsioris, K., Raja, W. K., Pritchard, E. M., Panilaitis, B., Kaplan, D. L., & Omenetto, F. G. (2012). Fabrication of Silk Microneedles for Controlled-Release Drug Delivery. *Advanced Functional Materials*, 22(2), 330-335. <https://doi.org/https://doi.org/10.1002/adfm.201102012>
- Uebersax, L., Mattotti, M., Papaloizos, M., Merkle, H. P., Gander, B., & Meinel, L. (2007). Silk fibroin matrices for the controlled release of nerve growth factor (NGF). *Biomaterials*, 28(30), 4449-4460. <https://doi.org/https://doi.org/10.1016/j.biomaterials.2007.06.034>
- Vincent, J. F. V. (2014). Chapter 17 - Biomimetic Materials. In E. Karana, O. Pedgley, & V.

- Rognoli (Eds.), *Materials Experience* (pp. 235-246). Butterworth-Heinemann.  
<https://doi.org/https://doi.org/10.1016/B978-0-08-099359-1.00017-5>
- Wang, H.-Y., & Zhang, Y.-Q. (2013). Effect of regeneration of liquid silk fibroin on its structure and characterization [10.1039/C2SM26945G]. *Soft Matter*, 9(1), 138-145.  
<https://doi.org/10.1039/C2SM26945G>
- Wang, X., Hu, X., Daley, A., Rabotyagova, O., Cebe, P., & Kaplan, D. L. (2007). Nanolayer biomaterial coatings of silk fibroin for controlled release. *J Control Release*, 121(3), 190-199. <https://doi.org/10.1016/j.jconrel.2007.06.006>
- Wang, X., Zhang, X., Castellot, J., Herman, I., lafrati, M., & Kaplan, D. L. (2008). Controlled release from multilayer silk biomaterial coatings to modulate vascular cell responses. *Biomaterials*, 29(7), 894-903.  
<https://doi.org/10.1016/j.biomaterials.2007.10.055>
- Wenk, E., Merkle, H. P., & Meinel, L. (2011). Silk fibroin as a vehicle for drug delivery applications. *Journal of Controlled Release*, 150(2), 128-141.  
<https://doi.org/https://doi.org/10.1016/j.jconrel.2010.11.007>
- Yang, M.-H., Chung, T.-W., Lu, Y.-S., Chen, Y.-L., Tsai, W.-C., Jong, S.-B., Yuan, S.-S., Liao, P.-C., Lin, P.-C., & Tyan, Y.-C. (2015). Activation of the Ubiquitin Proteasome Pathway by Silk Fibroin Modified Chitosan Nanoparticles in Hepatic Cancer Cells. *International Journal of Molecular Sciences*, 16(1), 1657-1676.  
<https://www.mdpi.com/1422-0067/16/1/1657>
- Yavuz, B., Zeki, J., Taylor, J., Harrington, K., Coburn, J. M., Ikegaki, N., Kaplan, D. L., & Chiu, B. (2019). Silk Reservoirs for Local Delivery of Cisplatin for Neuroblastoma Treatment: In Vitro and In Vivo Evaluations. *Journal of Pharmaceutical Sciences*, 108(8), 2748-2755. <https://doi.org/https://doi.org/10.1016/j.xphs.2019.03.019>
- Yucel, T., Lovett, M. L., Giangregorio, R., Coonahan, E., & Kaplan, D. L. (2014). Silk fibroin rods for sustained delivery of breast cancer therapeutics. *Biomaterials*, 35(30), 8613-8620. <https://doi.org/10.1016/j.biomaterials.2014.06.030>
- Zhang, L., Herrera, C., Coburn, J., Olejniczak, N., Ziprin, P., Kaplan, D. L., & LiWang, P. J. (2017). Stabilization and Sustained Release of HIV Inhibitors by Encapsulation in Silk Fibroin Disks. *ACS Biomaterials Science & Engineering*, 3(8), 1654-1665.  
<https://doi.org/10.1021/acsbomaterials.7b00167>

- Zhang, Y., Sun, T., & Jiang, C. (2018). Biomacromolecules as carriers in drug delivery and tissue engineering. *Acta Pharmaceutica Sinica B*, 8(1), 34-50.  
<https://doi.org/https://doi.org/10.1016/j.apsb.2017.11.005>
- Zhong, T., Jiang, Z., Wang, P., Bie, S., Zhang, F., & Zuo, B. (2015). Silk fibroin/copolymer composite hydrogels for the controlled and sustained release of hydrophobic/hydrophilic drugs. *International Journal of Pharmaceutics*, 494(1), 264-270. <https://doi.org/https://doi.org/10.1016/j.ijpharm.2015.08.035>
- Zhou, C.-Z., Confalonieri, F., Jacquet, M., Perasso, R., Li, Z.-G., & Janin, J. (2001). Silk fibroin: Structural implications of a remarkable amino acid sequence. *Proteins: Structure, Function, and Bioinformatics*, 44(2), 119-122.  
<https://doi.org/https://doi.org/10.1002/prot.1078>
- Zuluaga-Vélez, A., Cómbita-Merchán, D. F., Buitrago-Sierra, R., Santa, J. F., Aguilar-Fernández, E., & Sepúlveda-Arias, J. C. (2019). Silk fibroin hydrogels from the Colombian silkworm *Bombyx mori* L: Evaluation of physicochemical properties. *PLOS ONE*, 14(3), e0213303. <https://doi.org/10.1371/journal.pone.0213303>



จุฬาลงกรณ์มหาวิทยาลัย  
**CHULALONGKORN UNIVERSITY**



## VITA

**NAME** Jaturong Promsuk

**DATE OF BIRTH** 11 November 1991

**PLACE OF BIRTH** Phuket

**INSTITUTIONS ATTENDED** Bachelor of Science in Chemistry (Second class honor),  
Prince of Songkla University

**HOME ADDRESS** 88/203 The Empire Place, Narathiwat Ratchanakharin Rd.  
Yan Nawa, Sathon, Bangkok, 10120.

